Hydroxyurea Induces Cytokinesis Arrest in Cells Expressing a Mutated Sterol-14α-Demethylase in the Ergosterol Biosynthesis Pathway

Yong-jie Xu,*,[1] Amanpreet Singh,*,[2] and Gerald M. Alter†
*Department of Pharmacology and Toxicology and †Department of Biochemistry and Molecular Biology, Boonshoft School of Medicine, Wright State University, Dayton, Ohio 45435

ABSTRACT Hydroxyurea (HU) has been used for the treatment of multiple diseases, such as cancer. The therapeutic effect is generally believed to be due to the suppression of ribonucleotide reductase (RNR), which slows DNA polymerase movement at replication forks and induces an S phase cell cycle arrest in proliferating cells. Although aberrant mitosis and DNA damage generated at collapsed forks are the likely causes of cell death in the mutants with defects in replication stress response, the mechanism underlying the cytotoxicity of HU in wild-type cells remains poorly understood. While screening for new fission yeast mutants that are sensitive to replication stress, we identified a novel mutation in the *erg11* gene encoding the enzyme sterol-14α-demethylase in the ergosterol biosynthesis pathway that dramatically sensitizes the cells to chronic HU treatment. Surprisingly, HU mainly arrests the *erg11* mutant cells in cytokinesis, not in S phase. Unlike the reversible S phase arrest in wild-type cells, the cytokinesis arrest induced by HU is relatively stable and occurs at low doses of the drug, which likely explains the remarkable sensitivity of the mutant to HU. We also show that the mutation causes sterol deficiency, which may predispose the cells to the cytokinesis arrest and lead to cell death. We hypothesize that in addition to the RNR, HU may have a secondary unknown target(s) inside cells. Identification of such a target(s) may greatly improve the chemotherapies that employ HU or help to expand the clinical usage of this drug for additional pathological conditions.

KEYWORDS hydroxyurea; cytokinesis; the replication checkpoint; cell cycle; fission yeast

THE DNA replication checkpoint (DRC, also called the S phase checkpoint) is an intracellular signaling pathway that is activated in response to replication stress (Boddy and Russell 2001; Furuya and Carr 2003; Ciccia and Elledge 2010). Various factors such as nucleotide depletion, the damage of DNA templates, or polymerase inhibitors can perturb DNA replication and generate the replication stress. The activated DRC stimulates a series of protective cellular responses that promotes cell survival and prevents mutations from occurring under the stress conditions. In the absence of the DRC, perturbed replication forks collapse, which leads to chromosomal DNA damage or even cell death. Defects in the DRC are the known causes of genome instability, cancer, or other inherited diseases (Ahn *et al.* 2004; Stracker *et al.* 2008). Therefore, the DRC is crucial for the maintenance of genome stability and highly conserved in all eukaryotes.

DRC signaling is initiated at perturbed replication forks by the protein kinase ATR (ataxia telangiectasia and Rad3 related) facilitated by a few other sensor proteins that are also assembled at the chromosomal DNA associated with the forks. Activated ATR phosphorylates the mediator kinase CHK1 so that the checkpoint signal can be properly amplified and received by various cellular structures. The functional homolog of CHK1 in the fission yeast *Schizosaccharomyces pombe* is Cds1, although the structure of Cds1 is more closely related to mammalian CHK2 or *Saccharomyces cerervisiae* Rad53. Similar to the DRC signaling in mammalian cells, Cds1 is activated by the sensor kinase Rad3 (ATR/Mec1) and stimulates most of the protective cellular responses in *S. pombe*. Although the activation mechanisms of the mediator kinases Cds1 (Xu *et al.* 2006; Cai *et al.* 2009; Xu and Kelly 2009) and CHK1 (Chen *et al.* 2000;

doi: 10.1534/genetics.116.191536
Manuscript received May 12, 2016; accepted for publication August 18, 2016; published Early Online August 31, 2016.
Supplemental material is available online at www.genetics.org/lookup/suppl/doi:10.1534/genetics.116.191536/-/DC1.
[1]Corresponding author: Department of Pharmacology and Toxicology, Boonshoft School of Medicine, Wright State University, 3640 Colonel Glenn Hwy., Dayton, OH 45435. E-mail: yong-jie.xu@wright.edu
[2]Present address: Wadsworth Center, NYSDOH, 120 New Scotland Ave., Albany, NY 12208.

Han *et al.* 2016) have been well characterized, the mechanism by which the sensor kinases are activated under replication stress remains incompletely understood (Bandhu *et al.* 2014; Yue *et al.* 2014). Because fission yeast is an established model for studying the cellular mechanisms that are conserved in higher eukaryotes, we have been addressing this issue by searching for new *S. pombe* mutants that are sensitive to the replication stress induced by hydroxyurea (HU).

HU is a small molecule drug that has been used for multiple clinical implications and has a long history of scientific interest. It is a well-established inhibitor of the enzyme ribonucleotide reductase (RNR) that catalyzes the synthesis of deoxyribonucleotides from ribonucleotides. HU specifically quenches the catalytically important tyrosyl free radical within the small subunit of RNR and thus decreases the cellular dNTP levels. Consistent with this mechanism, HU slows replication forks and arrests the cell cycle in S phase (Krakoff *et al.* 1968; Ehrenberg and Reichard 1972; Nordlund and Reichard 2006). Slowed forks activate the DRC to up-regulate RNR and increase dNTP production, which promotes fork progression and therefore protects the forks from collapsing (Elledge *et al.* 1992; Lopes *et al.* 2001; Sogo *et al.* 2002; Hu *et al.* 2012). The activated DRC also delays mitosis and suppresses late firing origins so that DNA synthesis can properly resume after HU is removed (Lopez-Mosqueda *et al.* 2010; Zegerman and Diffley 2010). Thus, the DRC plays a key role in cell survival after HU challenge by preventing aberrant mitosis and DNA damage generated at collapsed forks, which are generally believed to be the direct causes of cell death in mutants with a defective DRC (Sogo *et al.* 2002; Hu *et al.* 2012). In support of this hypothesis, up-regulation of RNR small subunit, which has been observed in HU-resistant mammalian cell lines (Akerblom *et al.* 1981; Choy *et al.* 1988), suppresses the HU sensitivity of yeast DRC mutant cells. However, the mechanism by which HU kills wild-type cells with a functional DRC remains less clear. Although the DNA damage generated at collapsed forks may play an important role in the cell-killing process, direct evidence is still lacking.

Recent studies have shown that HU may kill the cells by alternative mechanisms such as by generating oxidative stress (Davies *et al.* 2009). Here, we report the identification of a novel mutation in the *erg11* gene in fission yeast, which is predicted to encode the essential enzyme sterol-14α-demethylase Erg11, a P450 enzyme in the ergosterol biosynthesis pathway (Turi and Loper 1992). The structure and the catalysis of Erg11 are highly conserved in human Cyp51 (Strushkevich *et al.* 2010). Interestingly, Erg11 is also a major therapeutic target of antifungals (Becher and Wirsel 2012). We found that the newly identified *erg11* mutation can dramatically sensitize the cells to chronic HU treatment. Surprisingly, unlike wild type or DRC mutants, in which HU induces an S phase cell cycle arrest, HU mainly arrests the *erg11* mutant cells in cytokinesis. Thus, these results clearly show that HU inhibits cell proliferation through a previously unknown mechanism. We propose that in addition to the primary target RNR, HU may have a secondary unknown target(s) inside the cell. Because HU has a long history of clinical use, understanding the novel cell-killing mechanism of HU may therefore greatly improve the HU-based chemotherapies.

Materials and Methods

Yeast strains and plasmids

Standard methods and genetic techniques were used for the yeast cell culture (Moreno *et al.* 1991). Yeast strains used in this study are listed in Supplemental Material, Table S1. The plasmids and PCR primers are listed in Table S2 and Table S3, respectively. To delete the *erg11* gene, *Xho*I and *Bam*HI sites were generated by PCR in the open reading frame (ORF) of *erg11* between 79 and 2568 bp from the start codon in the plasmid pYJ1519 (Figure S3A). After digestion with the two restriction enzymes, a 2489-bp fragment was removed from pYJ1519 by agarose gel electrophoresis and replaced with *ura4* marker to generate the deletion construct pYJ1526. The deletion construct was digested with *Bgl*II and *Pac*I to isolate the 3818-bp gene replacement fragment, which was transformed into the wild-type diploid strain YJ18. Colonies formed on EMM plates lacking uracil were screened by colony PCR to confirm the correct 5′ and 3′ integrations. The confirmed diploid strain was saved as YJ1245 and the essentiality of *erg11* was assessed by tetrad dissection (Figure S3A). A similar approach was used for integration of the *erg11-1* mutation at its genomic locus in the wild-type diploid strain YJ18 and subsequent tetrad dissection (Figure S3B). As a control, wild-type *erg11* was integrated using the same method. For experimental convenience, the *ura4* marker in the *erg11*Δ mutant YJ1259 strain was also replaced with KanRMX6 marker and saved as YJ1298.

Identification of erg11-1 mutant

Screening of new HU-sensitive (*hus*) mutants was carried out following a previously described method (Enoch *et al.* 1992). Briefly, the logarithmically growing wild-type TK1 strain was harvested and suspended in 50 mM Tris-maleate buffer, pH 6.0, and treated with 375 μg/ml methylnitronitrosoguanidine (MNNG) in the same buffer for 90 min at room temperature. MNNG is a potent carcinogen that alkylates genomic DNA at the O^6 of guanine and O^4 of thymine, leading to transition mutations between GC and AT. The TK1 cells were also mutagenized by treatment with 150 J/m^2 ultraviolet (UV) light (Stratalinker 2400) after the cells were filtered onto filter papers. The cells were washed twice after the mutagenesis with phosphate buffered saline (PBS), resuspended in EMM6S medium, and saved at 4°. For the *hus* screening, the mutagenized cells were spread on YE6S plates and incubated at 30°. The colonies were replicated onto YE6S plates containing HU to identify those that were sensitive to HU. The initially identified *hus* mutants were backcrossed three times to remove the bystander mutations. The resulting *hus* mutants were crossed and compared with all known checkpoint mutants and the mutants that are sensitive to HU to identify novel *hus* mutants. Preliminary characterization of one of our screened mutants

hus41 (Xu 2016) showed that this mutant contains a novel single nucleotide change in the *erg11* gene, which causes a G189D mutation in sterol 14α-demethylase (Figure 1). The *hus41* mutant was subsequently renamed as *erg11-1* mutant in this study.

Drug sensitivity

To test the drug sensitivity by spot assay, 2×10^7 cells/ml of logarithmically growing *S. pombe* were diluted in three- or fivefold steps and spotted onto YE6S plates or YE6S plates containing either HU or methyl methanesulfonate (MMS) at the indicated concentrations. The cells spotted on plates were also exposed to UV light at the indicated doses. All plates were incubated at 30° for 3 days and then photographed. The sensitivity of *S. pombe* to acute HU treatment was carried out using a standard method (Enoch *et al.* 1992). Briefly, after HU was added to the culture at a final concentration of 15 mM, an aliquot of the culture was removed every hour during the drug treatment, diluted 1000-fold in sterile deionized water, and spread onto YE6S plates. The plates were incubated at 30° for 3 days to allow the cells to recover. The colonies formed by the recovered cells were counted and presented as percentages relative to untreated cultures. Each data point represents the average of the numbers of colonies on three separate plates.

Western blotting

Phosphospecific antibodies against phosphorylated Mrc1-Thr^{645}, Cds1-Thr^{11}, and Rad9-Thr^{412} were generated using the chemically synthesized phosphopeptides (Xu *et al.* 2006; Xu and Kelly 2009). Rad9 and Cds1 were tagged with a hemagglutinin (HA) epitope and immunoprecipitated (IPed) from whole cell lysates prepared with the glass-bead method in a buffer containing 50 mM HEPES/NaOH (pH 7.6), 1 mM EDTA, 1 mM Na_3VO_4, 10 mM pyrophosphate, 50 mM NaF, 60 mM β-glycerophosphate, 0.1% Nonidet P-40, and protease inhibitors. After separation by SDS/PAGE, samples were transferred to a nitrocellulose membrane. The membrane was briefly probed with anti-HA antibody (Santa Cruz Biotechnology, Santa Cruz, CA) to show the HA-tagged proteins. The blotting signal was detected by electrochemiluminescence and photographed with an Image Reader LAS-3000 (Fujifilm, Tokyo, Japan). Band intensities were quantitated by using ImageGauge (Fujifilm). The blots were usually stripped by incubating at 70° for 30 min in the buffer containing 50 mM Tris:HCl (pH 7.5), 50 mM DTT, and 2% SDS. After extensive washes with distilled water, the stripped blots were blocked with 5% milk and reprobed with the phosphospecific antibodies in the presence of 5% milk for 3 hr at room temperature or overnight at 4°. Phosphorylation of Mrc1-Thr^{645} was directly examined in whole cell lysates prepared by the trichloroacetic acid (TCA) method (Xu *et al.* 2006). The stripped membranes were probed with polyclonal antibodies against Mrc1 to assess the loading. Phosphorylation of Chk1 by Rad3 was assessed using the standard mobility-shift method (Limbo *et al.* 2011).

Flow cytometry

The cells (0.5 OD_{600nm}) were collected by centrifugation and fixed in 1 ml of ice-cold 70% ethanol for ≥3 hr or overnight at 4°. The fixed cells were treated with 0.1 mg/ml RNase A in 50 mM sodium citrate at 37° for ≥5 hr and then stained with 4 μg/ml propidium iodide (PI). Stained cells were extensively vortexed and directly analyzed using an Accuri C6 flow cytometer. Collected data were analyzed by using FCS Express 4Flow software. The FL2-A channel was used for all histograms shown in this study.

Microscopy

The cells were fixed in 2.5% glutaraldehyde at 4° for ≥3 hr. After washing with PBS by centrifugation at 2300 × *g* for 30 sec, the fixed cells were stained in the same buffer containing 5 μg/ml of 4′,6-diamidino-2-phenylindole (DAPI) (Sigma-Aldrich, St, Louis, MO) and 1:100 dilution of the Blankophor working solution (1:1000 dilution of a stock solution, MP Biomedicals, Santa Ana, CA) for 5–10 min on ice. The stained cells were examined using an Olympus EX41 fluorescent microscope. Images were captured with an IQCAM camera (Fast1394) using Qcapture Pro 6.0 software. Individual images were extracted into Photoshop (Adobe) to generate the figures.

Data availability

The authors state that all data necessary for confirming the conclusions presented in the article are represented fully within the article.

Results

Identification of the new HU-sensitive mutant erg11-1

To better understand the checkpoint signaling at perturbed replication forks, we carried out a genetic screen in *S. pombe*, looking for novel mutants that are sensitive to the replication stress induced by HU (Enoch *et al.* 1992). After extensive crosses with all known mutants that are sensitive to HU, including all checkpoint mutants, this *hus* (HU sensitive) screen identified several new mutants that are highly sensitive to HU. In this paper, we report the characterization of one of our newly screened mutants that was initially described as *hus41* (Xu 2016). This mutant was subsequently renamed as *erg11-1* in this study after the identification of the mutation and the mutated gene (see below). Other newly screened *hus* mutants will be reported elsewhere.

The HU sensitivity of the initially screened *hus41* mutant was examined by standard spot assay and compared with known checkpoint mutants, including *rad3*, *cds1*, and *chk1* (Figure 1, A and D). We found that the mutant was highly sensitive to HU. The sensitivity was remarkable in that it was even slightly higher or equal to that of *rad3*, one of the most HU-sensitive mutants known so far in *S. pombe* (Figure 1D). Because of the remarkable sensitivity, we tested the HU from two different manufacturers and from various batch numbers

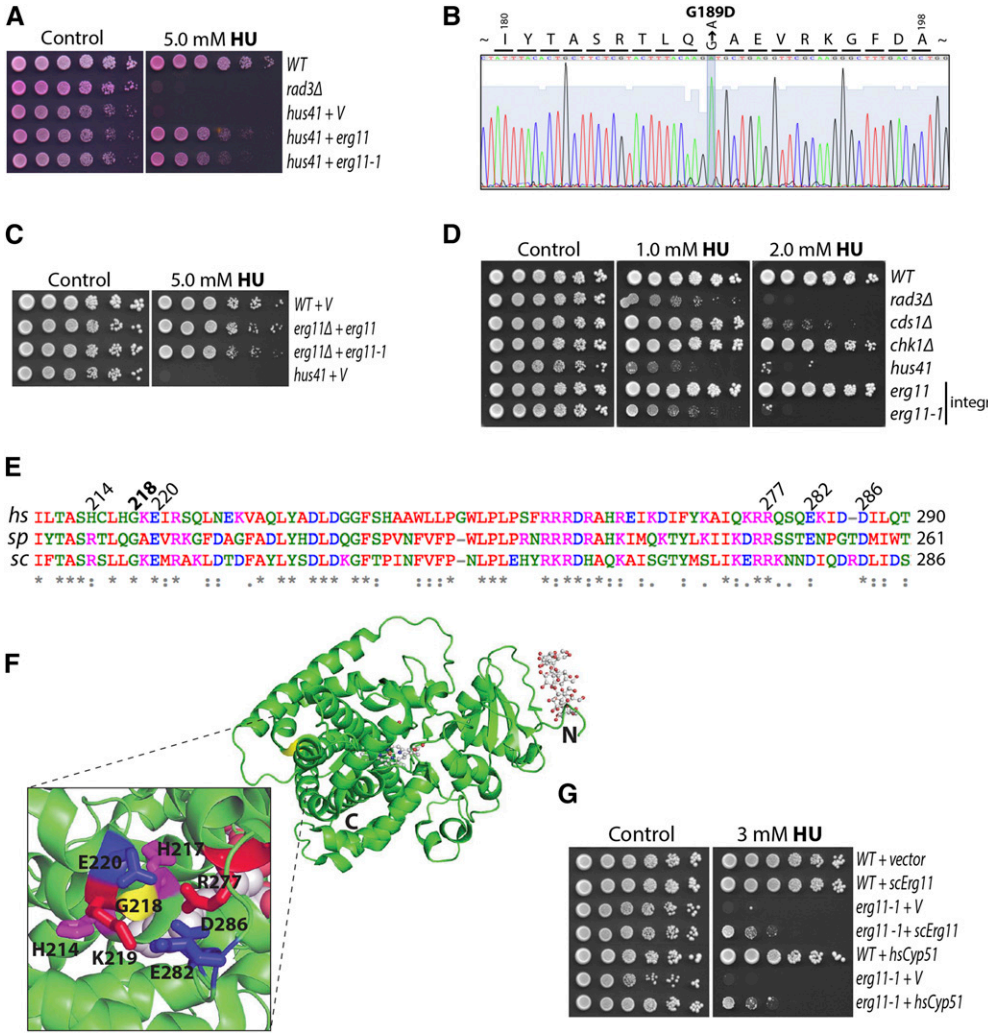

Figure 1 Identification of a hypomophic mutation in *erg11-1* that dramatically sensitizes *S. pombe* to chronic treatment with HU. (A) The newly screened *hus41* mutant was rescued by *erg11*. Standard spot assays were used to assess the HU sensitivity of wild type, *rad3*, and *hus41* carrying an empty vector (V), and *hus41* carrying the same vector expressing *erg11* or mutant *erg11-1* cloned from *hus41*. The 2×10^7 cells/ml of logarithmically growing *S. pombe* were diluted in fivefold steps and spotted onto YE6S plates as the control or YE6S plates containing 5.0 mM HU. The plates were incubated at 30° for 3 days before they were photographed. The dye Phloxin B was added to the medium in this experiment as the indicator of cell lethality. (B) DNA sequencing of the *erg11* cloned from *hus41* identified a single G-to-A mutation that causes G189D amino acid change in the enzyme. (C) Overexpression of mutant Erg11 in cells lacking the *erg11* gene generated minimal HU sensitivity as determined by standard spot assay. (D) Integration of mutant *erg11-1* in the *erg11* genomic locus sensitized *S. pombe* to HU to the same level as the *hus41* mutant. The *erg11-1* mutation was integrated at the genomic locus as illustrated in Figure S3. As a control, wild-type *erg11* was integrated by the same method. The HU sensitivity of the resulting integrants was assessed by spot assay and compared with that of wild-type, *rad3*, *cds1*, *chk1*, and *hus41* cells. (E) The mutated glycine residue in Erg11 is conserved from yeasts to humans. Regional amino acid sequences of human CYP51, *S. cerevisae*, and *S. pombe* Erg11 were aligned together using the numbering of the amino acids in human CYP51 (numbers on top). Number 218 is in boldface type to indicate the mutated glycine residue in *hus41*. The highly conserved two histidines and four charged residues surrounding the mutated glycine residue are also numbered. (F) The mutated residue is located outside the catalytic center. The crystal structure of human CYP51 is shown by POLYVIEW (Porollo *et al.* 2004). The N and C termini are marked by N and C, respectively. Also shown are cyclohepta-amylose co-crystalized with the N terminus and the inhibitor econazole that occupies the catalytic center (Strushkevich *et al.* 2010). The mutated region is enlarged to show the surrounding four charged residues and the two histidines numbered in E. (G) Overexpression of human CYP51 and *S. cerevisiae* Erg11 in *S. pombe* partially rescued the *erg11-1* mutant. HU sensitivity of wild-type or *erg11-1* mutant cells carrying an empty vector or the same vector expressing human Cyp51 or *S. cerevisiae* Erg11 was assessed by spot assay. Expression of the human Cyp51 and *S. cerevisiae* Erg11 was under the control of *nmt1* promoter.

to verify that the cell-killing effect was caused by HU and not by impurities. All of the samples had an indistinguishable cell-killing effect (Figure S1), which shows that the remarkable cytotoxicity was indeed caused by HU.

To identify the mutation in *hus41*, *S. pombe* genomic expression libraries were made using DNA purified from the wild-type strain TK1 (Table S1) and then transformed into the *hus41* cells to screen colonies with conferred HU resistance. After screening a total of ~40,000 yeast colonies, 11 such HU-resistant colonies were isolated. The plasmids were recovered from the isolated colonies and then subjected to digestion with restriction enzymes. The digestion results showed that the recovered plasmids carried two common pieces of genomic DNA. DNA sequencing showed that either the *erg11* gene encoding the predicted sterol-14α-demethylase or the *pof1* gene encoding an F-box/WD repeat protein might be able to confer the HU resistance in *hus41*. To confirm the result, we cloned the *erg11* and *pof1* genes from the TK1 strain and the *hus41* mutant, respectively, and expressed them on a vector in the *hus41* mutant cells. The results showed that, while *erg11* could almost fully rescue *hus41* (Figure 1A), *pof1* could not (Figure S2), indicating that *erg11* might be the gene that was mutated in *hus41*. Subsequent DNA sequencing identified a single G → A mutation that would cause a G189D amino acid change in the Erg11 enzyme (Figure 1B). We also sequenced the *pof1* gene cloned from the *hus41*

mutant; no mutation was found. Interestingly, although weaker than wild-type enzyme, the mutated Erg11 expressed on the vector could also rescue *hus41* (Figure 1A). Because the protein levels are usually higher when expressed from vectors that exist in multiple copies inside the cell, this result indicates that either the *erg11* mutation is hypomorphic or an unknown mutation remains to be identified in *hus41*.

To distinguish between these two possibilities, we deleted *erg11* in the wild-type diploid strain YJ18 by replacing it with the *ura4* marker (Figure S3A). Tetrad dissection showed that the deletion is lethal, which confirms a previous genome-wide deletion study (Kim *et al.* 2010). Expressing Erg11 ectopically on a vector conferred normal cell growth and HU resistance in *erg11*Δ haploid cells (Figure 1C). Interestingly, the *erg11*Δ cells expressing the mutated Erg11 were only slightly sensitive to HU. This result shows that the HU sensitivity was likely caused by a hypomorphic mutation in *hus41* and not by an unidentified mutation. We then fused the mutated *erg11* with the *ura4* marker and integrated it at its genomic locus in a wild-type strain (Figure S3B). All integrants showed the HU sensitivity similar to *hus41* such as the one shown in Figure 1D. In contrast, none of the integrants of wild-type *erg11* obtained by using the same method were sensitive to HU (Figure 1D). Furthermore, the DRC signaling in the integrated mutants was almost identical to that in the *hus41* cells (Figure S4). To confirm the overexpression of Erg11 in cells containing an expression vector, we tagged the wild-type and the mutant enzyme with a triple HA epitope at the C terminus and expressed the tagged enzyme from the genomic locus or from a vector in the *erg11*Δ cells. We found that the protein level of Erg11 expressed from the vector was about four-fold higher than that expressed from the genomic locus (Figure S5). Together, we have identified a hypomorphic mutation in *erg11* that dramatically sensitizes *S. pombe* to the clinically used drug HU. In the rest of this study, the *hus41* mutant was therefore renamed as *erg11-1*.

The conserved function of Erg11 in sterol synthesis

Erg11 is a P450 enzyme that catalyzes the key step, lanosterol-14α-demethylation, in the biosynthesis of ergosterol, a sterol that is similar to mammalian cholesterol and specifically found in fungal cell membranes (Turi and Loper 1992; Espenshade and Hughes 2007). The structure and the catalysis of Erg11 are conserved in human Cyp51 with a subtle difference in the substrates. For this reason, it is one of the major targets of antifungal agents (Becher and Wirsel 2012). It was therefore a surprise that our screen identified an *erg11* mutation that dramatically sensitizes the cells to HU. The mutated glycine residue in Erg11 is absolutely conserved from yeasts to humans (Figure 1E). Interestingly, based on the crystal structure of human Cyp51, the mutated residue is located outside of the catalytic center, which is consistent with the hypomorphic mutation and suggests that the catalysis may not be seriously affected. Because the mutated glycine is surrounded by three negatively charged, two positively charged, and two histidine residues (Figure 1F), it is possible that mutation to the negatively charged aspartic acid may perturb the local protein structure and thus decrease the enzymatic activity (Lamb *et al.* 1999). Because all of these residues are highly conserved (Figure 1E), it is also possible that the same mutation in other eukaryotes may have a similar effect. To test this hypothesis, we overexpressed the *S. cerevisiae* Erg11 and human Cyp51 in wild-type or mutant *S. pombe* (Figure 1G). The results showed that under normal conditions, overexpression of the homologous enzymes did not affect cell growth in *S. pombe*. Interestingly, both the *S. cerevisiae* and human enzymes could partially rescue the HU sensitivity of the *erg11-1* cells, which suggests that the enzyme is highly conserved. We also introduced the same G-to-D mutation in the human and *S. cerevisiae* enzymes and found that the mutated enzymes could also partially rescue the *erg11-1* mutant (Figure S6). This result is consistent with the hypomorphic mutation and further supports our notion that overexpression can overcome the partial defect of Erg11.

Reduced DRC signaling in the presence of HU

The HU sensitivity described above suggests that the mutation may cause a defect in the DRC, which subsequently leads to cell death. We therefore examined the DRC signaling from Rad3 to Mrc1 (human Claspin) and Cds1 using Western blotting with phosphospecific antibodies (Figure 2). We have previously shown that in the presence of HU, two TQ motifs containing Thr^{645} and Thr^{653} residues in Mrc1 are phosphorylated by Rad3 in *S. pombe*. Once phosphorylated, the two TQ motifs function redundantly in recruiting Cds1 to be phosphorylated by Rad3 (Xu *et al.* 2006). As shown in Figure 2A, when wild-type cells were treated with HU, Thr^{645} in Mrc1, a representative of the two threonine residues in the redundant TQ motifs, was highly phosphorylated. Deletion of *rad3* completely eliminated the phosphorylation, which is consistent with Rad3-dependent phosphorylation (compare *rad3*Δ with wild-type and *mrc1*Δ cells). In HU-treated *erg11-1* cells, however, the Mrc1 phosphorylation was reduced to ~67% of the level in wild-type cells. Interestingly, the protein level of Mrc1 was also significantly lower in the HU-treated *erg11-1* cells (Figure 2A, 2nd panel from the top), which may provide an explanation for the reduced phosphorylation. To confirm the result, we compared the Mrc1 phosphorylation in *hus41* with that in cells with the integrated *erg11-1* mutation and found that the results were almost identical (Figure S4). We then examined Mrc1 phosphorylation at various time points during the HU treatment (Figure 2B). The results clearly showed that unlike the wild-type cells in which the Mrc1 level was significantly increased by HU treatment, the Mrc1 protein remained at a low level in *erg11-1* cells during the 5-hr-long HU treatment. Since the transcription factor Cdc10 that regulates the expression of Mrc1 is a target of DRC (Ivanova *et al.* 2013), the low Mrc1 level might be due to a checkpoint defect. Alternatively and as it is shown below, the low level of Mrc1 was likely caused indirectly by a cell cycle defect.

We next examined the phosphorylation of Rad9 in the 9-1-1 checkpoint clamp complex (Figure 2C). In the presence of HU,

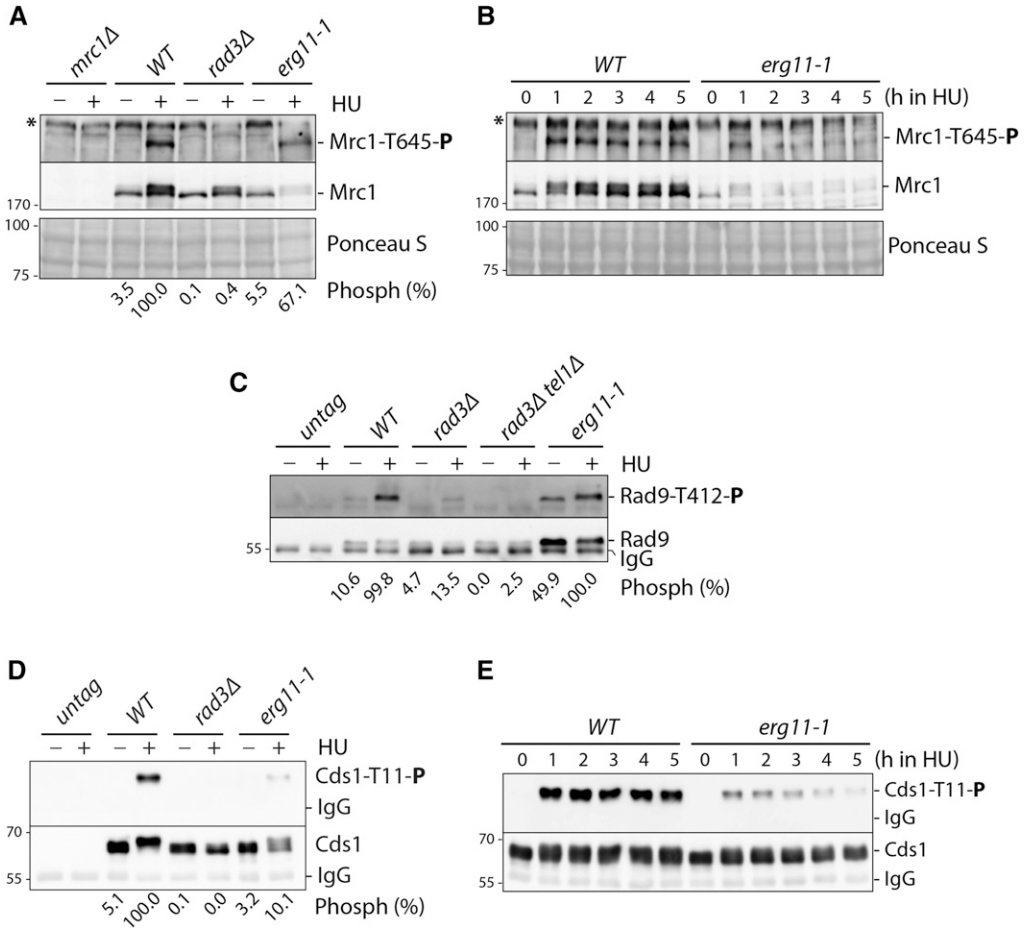

Figure 2 Reduced DRC signaling in the *erg11-1* mutant. (A) Wild-type, *erg11-1*, and cells lacking Mrc1 or Rad3 were incubated with (+) or without (−) 15 mM HU at 30° for 3 hr in YE6S medium. An equal number of cells was collected for preparation of the whole cell extracts as described in *Materials and Methods*. After separation by SDS/PAGE, the phosphorylation of Mrc1-Thr^{645} by Rad3 was examined by Western blotting using a phosphospecific antibody (top). The asterisk on the left denotes a nonspecific, cross-reactive material. The membrane was stripped and reprobed with the polyclonal antibodies against Mrc1 (middle). A section of the Ponceau S-stained membrane is shown as a loading control (bottom). The relative levels of phosphorylation were quantitated and are shown on the bottom. (B) Mrc1 phosphorylation was examined at the indicated time points during the course of HU treatment. (C) Rad9 was tagged with HA at the N terminus and expressed from the endogenous locus in *erg11-1* or the indicated checkpoint mutant cells. After the cells were treated with 15 mM HU at 30° for 3 hr in YE6S medium, extracts were made from an equal number of the cells. Rad9 was IPed with anti-HA antibody from the cell extracts. After separation by SDS/PAGE, phosphorylated Rad9-Thr^{412} was detected by Western blotting using the phosphospecific antibodies (top). Untagged cells were used as the control for HA-specific IPs (two lanes on the left). The same membrane was stripped and reprobed with the anti-HA antibody to reveal the tagged Rad9 (bottom). Relative phosphorylation levels are shown at the bottom. (D) Cds1 was tagged with HA epitope at the C terminus and expressed at the *cds1* genomic locus in wild-type, *erg11-1*, or cells lacking Rad3. After the cells were treated with 15 mM HU for 3 hr in YE6S medium, the phosphorylation of Cds1-Thr^{11} was assessed in IPed Cds1 by Western blotting (top). The same membrane was stripped and reprobed with anti-HA antibody to examine Cds1 (bottom). Phosphorylation levels in various mutants are shown on the bottom. (E) The phosphorylation of Cds1-Thr^{11} was examined at the indicated time points during the course of HU treatment.

Rad3 also phosphorylates Thr^{412} in the Rad9 C-terminus (Furuya *et al.* 2004) to facilitate the phosphorylation of Cds1. Tel1 (ATM in humans), the second sensor kinase in *S. pombe*, which is not required for cell survival in HU, also phosphorylates Rad9. However, double depletion of Rad3 and Tel1 completely eliminated the Rad9 phosphorylation (compare *rad3*Δ mutant with the *rad3*Δ *tel1*Δ double mutant). Interestingly, Rad9 phosphorylation was not affected by the *erg11-1* mutation. Furthermore, in contrast to Mrc1, the protein level of Rad9 was higher in the mutant even in the absence of the HU treatment.

The major DRC mediator Cds1 in *S. pombe* is activated by a two-stage mechanism (Xu *et al.* 2006; Xu and Kelly 2009; Yue *et al.* 2011). In the first stage, Cds1 is recruited by phosphorylated Mrc1 to be phosphorylated by Rad3 at the Thr^{11} residue. In the second stage, phosphorylated Cds1-Thr^{11} promotes homodimerization of two inactive Cds1 molecules, which facilitates the autophosphorylation of Thr^{328} in the kinase domain. Phosphorylation of Thr^{328} directly activates Cds1. Because the phosphorylation of Cds1-Thr^{11} by Rad3 primes autoactivation of the kinase, it has been used as a reliable marker for Cds1 activation (Tanaka *et al.* 2001; Yue *et al.* 2011). As shown in Figure 2D, the phosphorylation of Cds1-Thr^{11} was significantly increased in HU-treated wild-type cells and the phosphorylation was dependent on Rad3. Interestingly, phosphorylation of Cds1-Thr^{11} was significantly decreased in the *erg11-1* mutant cells. Quantitation results showed that only ~10% of the phosphorylation remained in the HU-treated mutant cells (Figure 2D, bottom). Our time course study showed that Cds1 phosphorylation remained at a low level during the 5-hr-long HU treatment (Figure 2E).

Minimal sensitivity to acute HU treatment and DNA damage

The HU sensitivity determined with the standard spot assay involves a chronic drug treatment of ~3 days. Because the DRC mutants are sensitive to HU under various conditions, the remarkable HU sensitivity determined by spot assay

prompted us to examine whether the *erg11-1* mutant is also sensitive to acute HU treatment (Figure 3A). Surprisingly, unlike the *rad3* and *cds1* mutants, which died within ~3 hr or ~1 cell cycle time after HU was added to the medium, the *erg11-1* mutant was relatively insensitive during the course of HU treatment. However, unlike wild-type cells that continued to grow in the presence of HU, the cell growth of the *erg11-1* mutant was completely suppressed.

One of the major functions of the DRC is to protect perturbed forks against collapse. Consistent with this notion, the DNA damage checkpoint (DDC) is activated in HU-treated cells that lack a functional DRC, probably due to the DNA damage caused by fork collapsing. As shown in Figure 3B, the major mediator of the DDC pathway, Chk1, was highly phosphorylated in HU-treated *cds1* mutant (Limbo *et al.* 2011), which suggests the presence of collapsed forks (Lindsay *et al.* 1998; Noguchi *et al.* 2003). In contrast, under similar conditions, Chk1 was only minimally phosphorylated in *erg11-1* cells. These results suggest that similar to wild-type cells, the HU-treated forks rarely collapse in the mutant.

We also used the standard spot assay to examine the sensitivity of *erg11-1* cells to DNA damage induced by MMS or UV light (Figure S7A). Unlike the DDC checkpoint *rad3* and *chk1* mutants that are highly sensitive to MMS and UV, the *erg11-1* mutant showed only a minimal sensitivity. The *cds1* mutant is not very sensitive to DNA damage, consistent with its main function in the DRC, not in the DDC. We then treated the cells in liquid cultures with MMS for various time points and found that the *erg11-1* mutant was only minimally sensitive (Figure S7B). We then examined the Chk1 activation in MMS-treated *erg11-1* cells (Figure S7C). In the presence of MMS, Chk1 was highly phosphorylated in wild-type cells and the phosphorylation absolutely required Rad3. Depletion of Cds1, the major mediator of DRC, further increased the Chk1 phosphorylation. Consistent with the minimal sensitivity to DNA damage, Chk1 phosphorylation was slightly affected in *erg11-1* mutant. These results clearly showed that the *erg11-1* mutant was relatively insensitive to acute HU treatment and DNA damage, and that the DDC signaling remained largely intact.

The checkpoint signaling defect may not play a major role in sensitizing the erg11-1 cells to HU

The results described above suggest that the defect in the activation of Mrc1 and Cds1 by Rad3 may sensitize the cells to HU. However, the insensitivity to acute HU treatment and DNA damage suggests an alternative mechanism. To further investigate, we examined whether the *erg11-1* mutant could be rescued by overexpression of Suc22, the small subunit of RNR. As mentioned above, in the presence of HU, one of the major functions of the DRC is to stimulate RNR so that more dNTPs are produced for DNA synthesis. Because Suc22 is the major DRC regulation target (Fernandez Sarabia *et al.* 1993; Nestoras *et al.* 2010), overexpression of Suc22 rescued the DRC mutants, including *rad3*, *mrc1*, and *cds1* (Figure 3C). Interestingly, under similar conditions, overexpression of

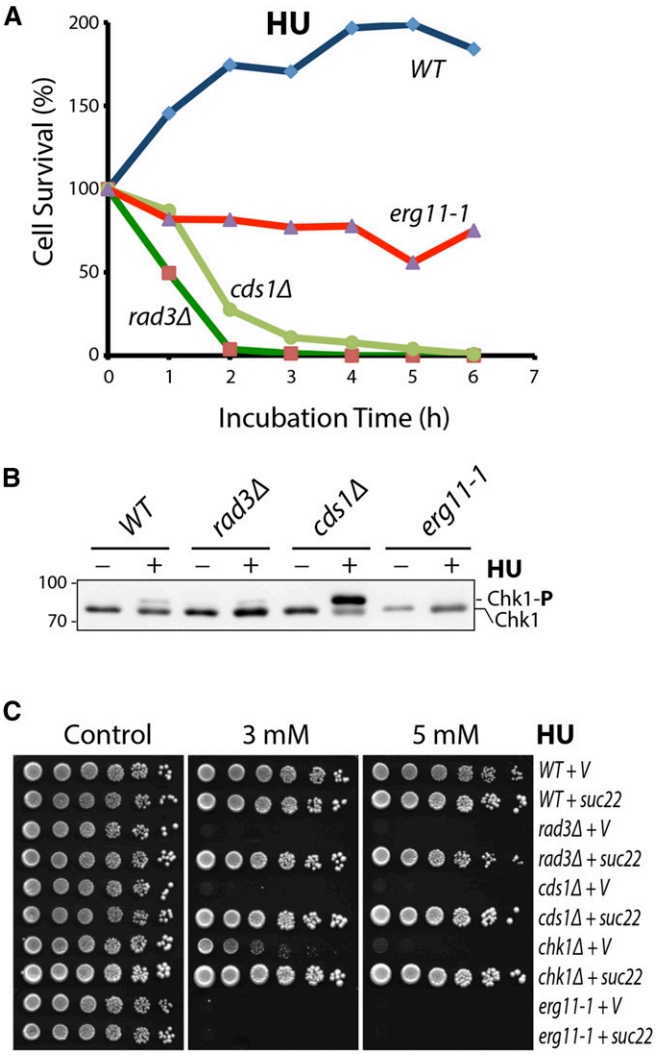

Figure 3 The *erg11-1* mutant is minimally sensitive to the acute treatment of HU. (A) Sensitivity of wild-type, *rad3*, *cds1*, and *erg11-1* mutant cells to acute treatment with HU was examined as described in *Materials and Methods*. After HU was added to the cultures at 15 mM, an equal amount of the culture was removed, diluted 1000-fold, and spread on YE6S plates to allow the cells to recover. The colonies formed from the recovered cells were counted and presented as the percentages relative to the untreated cultures. (B) Chk1 is minimally phosphorylated in the HU-treated *erg11-1* mutant. Chk1 phosphorylation was assessed in cells containing the indicated mutations treated with (+) or without (−) 15 mM HU at 30° for 3 hr. (C) Unlike the *rad3*, *cds1*, and *chk1* checkpoint mutants, overexpression of the small subunit of RNR Suc22 did not rescue the *erg11-1* mutant. Suc22 was expressed under the control of its own promoter from a vector carrying the LEU2 marker. V, empty vector. Standard spot assay was employed for assessing the HU sensitivity.

Suc22 did not rescue the *erg11-1* mutant, which suggests that the reduced DRC signaling may not be the major cause of lethality in HU-treated *erg11-1* cells. We also crossed the *erg11-1* mutation into the known checkpoint mutants to generate double mutants and examined the sensitivity of the resulting double mutants to HU, MMS, and UV (Figure S8). The results showed that the *erg11-1* mutation has a dominant effect over the checkpoint mutants in sensitizing the cells to

HU and the DNA damage caused by MMS or UV, which is consistent with our notion that the checkpoint defect may not contribute significantly to cell death in the *erg11-1* mutant.

HU arrests the erg11-1 cells mainly in cytokinesis, not in S phase of the cell cycle

Because Mrc1 is specifically expressed during early S phase, the DRC is functional only when the cells pass the G1/S transition. Outside of the S phase, the DDC is activated in the presence of DNA damage. The checkpoint signaling defect described above, in particular, the decreased Mrc1 protein level, may be caused by an indirect cell cycle effect. In support of this hypothesis, the cell growth of the *erg11-1* mutant was completely suppressed in the presence of HU (Figure 3A). We therefore analyzed the cell cycle progression by flow cytometry during a standard HU block and release. As shown in Figure 4A, when wild-type cells were treated with 15 mM HU for 3 hr, most of the cells were arrested with a 1C DNA content, which is consistent with a S phase arrest. After the cells were released into fresh medium, the cells finished the bulk of DNA synthesis within ~2 hr and then moved onto the next cycle in ~2.5 hr. After a 3-hr release, the cell cycle returned back to normal. Although the *rad3* checkpoint mutant was also arrested by HU with a 1C DNA content, the cells could not recover from the arrest after the release (Figure 4A, middle column). Interestingly, most of the *erg11-1* cells were not arrested in G1/S phase by HU. Instead, they remained at G2/M during the 3-hr-long HU treatment. After the HU removal, a large percentage of the cells moved onto 4C DNA content, which suggests a defect in cell separation and is inconsistent with the DRC signaling defect described above.

We then stained the cells with PI and Blankophor for DNA and cell wall/septum, respectively, and examined the cells by fluorescence microscopy (Figure 4B). Unlike the HU-treated wild-type cells that contained only one nucleus, the majority of the *rad3* cells had a septum and an unequal distribution of the genomic DNA. This so-called "cell untimely torn" (*cut*) cell phenotype is a strong indicator of a checkpoint defect (Saka and Yanagida 1993) and the likely cause of cell death of checkpoint mutants in HU (arrows in Figure 4B). Interestingly, a large number of HU-treated *erg11-1* cells contained two nuclei separated by a brightly stained septum (Figure 4B, right). This result is consistent with the flow cytometry data and shows that the cells were arrested by HU in cytokinesis and not in S phase. The septation index was determined during the course of the HU block and release (Figure 4C). When wild-type cells were treated with HU, the index went down from >20 to ≤5% because the activated DRC delays mitosis. After the release, the cell cycle resumed with the septation peaking at 2.5 hr after the release. In contrast, when *rad3* cells were treated with HU, the index went up and continued to go up to ≥60% after the release. Interestingly, after HU was added to *erg11-1* cells, the septation index went up immediately to >40% and remained at this high level even after the drug was removed, which indicates that HU mainly arrests the cells in cytokinesis in a relatively stable manor and the cytokinesis arrest appears to be a separate event unrelated to the S phase arrest.

HU induces a cytokinesis arrest at low doses

Cytokinesis is the final stage of the cell division cycle and requires the proper placement, assembly, and contraction of the contractile ring, which dictates septum formation and cell separation (Bathe and Chang 2010; Johnson *et al.* 2012; Lee *et al.* 2012). The HU-induced cytokinesis observed in *erg11-1* cells is likely a new cell-killing mechanism of this clinically important drug. One concern is that the cytokinesis arrest is caused by increased membrane permeability because of a defect in sterol synthesis, although the MMS resistance described above suggests that this is unlikely. To investigate this possibility, we treated the cells with HU at a wide range of concentrations from 1.5 to 50 mM. In wild-type and *rad3* cells, S phase arrest became apparent only when the drug concentration reached ≥6.3 mM (Figure 5A). Below this level, the cell cycle was not arrested. In contrast, the majority of the *erg11-1* cells were arrested with a 4C DNA content even at 1.5–3.1 mM of HU (arrows in Figure 5A), which is much lower than the concentration required for the S phase arrest in wild-type and the *rad3* cells. When the drug concentration was increased to ≥6.3 mM, most of the *erg11-1* cells were blocked with a 2C DNA content, probably because cytokinesis and DNA replication were both arrested. Further increasing the HU concentration up to 50 mM, the mutant cells remained with a 2C DNA content. Interestingly, a large number of wild-type cells also arrested in 2C DNA content at 50 mM HU, which is suggestive of a G2/M arrest. However, Blankophor staining showed that these cells were not arrested in cytokinesis (data not shown).

We then examined the cells treated with low doses of HU. Using bright field microscopy, the untreated *erg11-1* cells appeared similar to *rad3* and wild-type cells (Figure 5B, 1st column from the left). These results were confirmed by Blankophor staining (Figure 5B). After a 3-hr treatment with 3.1 mM HU, wild-type and *rad3* cells were morphologically similar to the untreated cells, which confirms that HU had no noticeable effects at this concentration. However, under similar conditions, the *erg11-1* cells appeared morphologically distinct from the untreated *erg11-1* as well as the wild-type and *rad3* cells (bottom). Most of the cells appeared to have vacuole-like structures and an enlarged nucleus (Figure 5B and Figure S9). Under the fluorescent microscope, ≥50% cells in the culture were found to contain a brightly stained septum, which confirms that the cytokinesis arrest was induced by HU at the concentrations where it has a minimal effect on DNA replication in both wild-type and *rad3* cells.

The cells containing a Blankophor-stained septum were counted in HU-treated and untreated cultures (Figure 5C). Before HU was added, ~18% of the cells had a septum in both wild-type and *rad3* cells, whereas the separation index was slightly higher in *erg11-1* culture. However, after the cells were treated with 1.5–3.1 mM HU for 3 hr, the index went up to ≥50% in *erg11-1* mutant. At these low doses, HU had

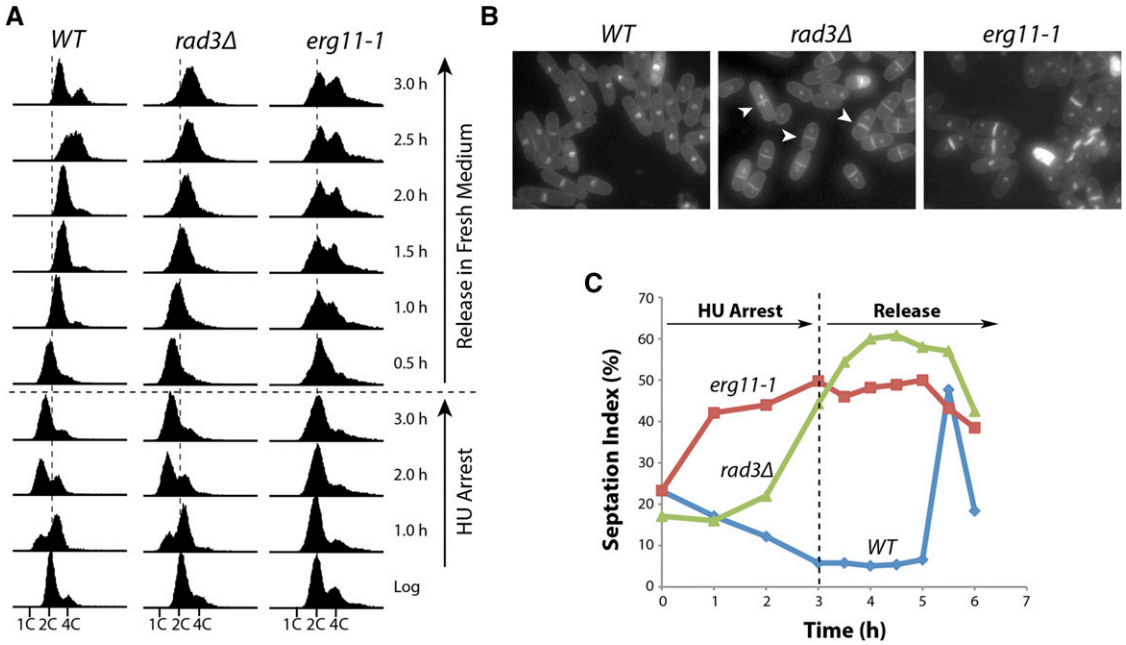

Figure 4 HU induces cytokinesis arrest in *erg11-1* cells. (A) Cell cycle progression of wild-type, *rad3*, and *erg11-1* cells during the HU block-and-release experiment were examined at the indicated time points by flow cytometry. 1C, 2C, and 4C indicate the DNA contents. (B) Wild-type, *rad3*Δ, and the *erg11-1* mutant cells were treated with HU for 3 hr, stained with PI and Blankophor, and examined under the microscope. Arrowheads indicate cells with a *cut* phenotype, which is an indicator of aberrant mitosis in *rad3* cells. (C) Cells with a septum were counted in cultures containing wild-type, *rad3*Δ, and *erg11-1* cells at the indicated time points during the HU block-and-release experiments. The results are shown as the percentages relative to untreated cultures. All data points are the averages of three independent samples.

little effect on wild-type and *rad3* cells, although the index in wild-type cells was slightly lower. When drug concentration was increased to ≥6.3 mM, the index in *rad3* cells began to increase to ≥50% and stayed at this high level after HU concentration was further increased. Under similar conditions, the index in wild-type cells went down to ≤2%, consistent with the DRC activation and the S phase arrest shown in Figure 4C. Interestingly, further increasing the drug concentrations to ≥6.3 mM decreased the index to <40% in *erg11-1* cells. We believe that the decreased septation index in presence of higher concentrations of HU is likely caused by the S phase arrest, which is consistent with the results shown in Figure 4, in which the cytokinesis arrest is induced by a mechanism different from that in the S phase arrest. Together, these results clearly showed that the HU-induced cytokinesis arrest was not caused by increased membrane permeability.

The cytokinesis arrest is relatively stable

The cytokinesis arrest induced by HU at low doses may explain the dramatic sensitivity of *erg11-1* to chronic HU treatment. However, a transient cell cycle arrest may not be harmful enough to cause lethality. For example, most of wild-type cells can fully recover from the HU-induced S phase arrest (Figure 3A). We next examined whether the HU-induced cytokinesis arrest in *erg11-1* cells is stable. In *S. pombe*, G2 is the longest phase of the cell cycle. As a result, most of the logarithmically growing haploid cells have a 2C DNA content. Because the cytokinesis arrest and the S phase block are separate events and via different mechanisms in the *erg11-1* mutant, we reasoned that if the cytokinesis arrest is transient, the released cells should be arrested in S phase in the presence of HU, which can easily be detected by flow cytometry as the cells with a 1C DNA content. To better arrest the cells in S phase, HU concentration was increased to 25 mM in this experiment. As shown in Figure 6B, when HU was added to wild-type cells, almost all cells were arrested in S phase in ≤3 hr. Although the DNA synthesis continued in the presence of HU, the S phase arrest remained apparent for at least 5 hr after the HU was added. However, during the 8-hr-long HU treatment, the cells with a 1C DNA content were hardly observed in *erg11-1* mutant. Interestingly, the vacuole-like structures began to appear at 0.5 hr and became apparent at 1 hr after HU was added (Figure 6A). Unlike wild-type cells that were significantly elongated during the later hours of HU treatment, the length of *erg11-1* cells hardly changed during the course of drug treatment. Because of the continued cell growth of wild-type cells in HU and uncertainty of drug decomposition, the HU treatment was stopped at 8 hr. Interestingly, unlike wild-type cells that could almost fully recover in 20 hr from the 8-hr-long HU arrest, the mutant cells could not (Figure 6C). This result showed that the HU-induced cytokinesis arrest is relatively stable in comparison to the S phase arrest. Longer exposures even at low doses as in the spot assay may induce irreversible arrest and lead to cell death, which likely causes the remarkable HU sensitivity.

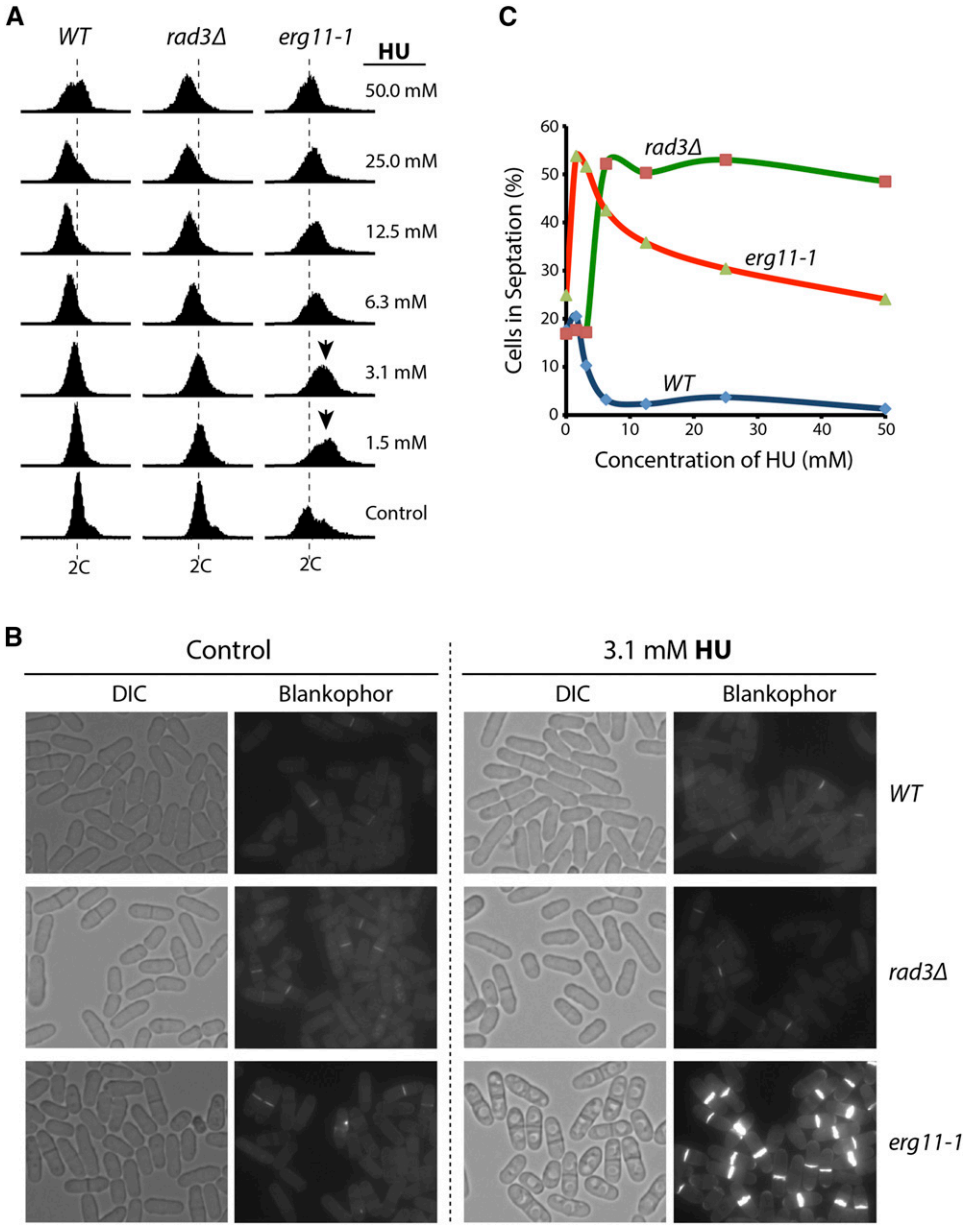

Figure 5 HU induces a cytokinesis arrest at low doses. (A) Logarithmically growing wild-type cells or cells with the indicated *rad3* or *erg11-1* mutation were incubated with HU for 3 hr at the indicated doses. Cell cycle distribution was analyzed by flow cytometry. Dashed lines indicate the cells with 2C DNA content. Arrows denote the cells with ≥2C DNA contents. (B) Cells were treated with 3.1 mM HU for 3 hr and then examined under the microscope. Untreated cells were marked as the control. The 1st and the 3rd columns from the left are the pictures taken in bright field while the 2nd and the 4th are the Blankophor-stained cells examined under fluorescent microscope. (C) Cells with a septum in the HU-treated cultures at the indicated concentrations were counted and are presented as the percentages of the untreated cultures. Each data point is the average of three samples.

The mutation may partially affect Cds1 activation

Since the DRC is activated only when DNA replication is perturbed, it is likely that the partial defect in Cds1 activation shown in Figure 2D is caused indirectly by a cell cycle effect, because in the presenceof HU, most of the mutant cells were arrested in G2/M, not in S phase (Figure S10, right column). Consistent with this, the Mrc1 level remained low during the HU treatment and the mutant cells were not sensitive to acute HU treatment (Figure 2B and Figure 3A). To investigate this further, we crossed the *erg11-1* mutation into the *cdc10-129 ts* mutant. As mentioned above, Cdc10 is a transcription factor required for G1/S transition and the expression of Mrc1 in *S. pombe*. When cultured at 36.5°, the *cdc10-129* cells arrest in G1, which allowed the release of the arrested cells into S phase at the permissive temperature of 25° in the presence or absence of HU (Lowndes *et al.* 1992). In this way, almost all *erg11-1* cells will be arrested in S phase by HU, which excludes the indirect cell cycle effect on Cds1 activation. As shown in Figure S11A, when *cdc10-129* or wild-type cells were cultured at 36.5° for 4 hr, the majority of the cells were arrested at G1. After release at 25° in fresh medium, the cells returned to the cycle. After a 5-hr release, the cell cycle returned back to normal. In the presence of HU, the G1 released cells were arrested in S phase for ≥5 hr. The *erg11-1* cells were also arrested at G1 by culturing at 36.5° and then released into S phase at 25°, although the release appeared to be slightly slower than the wild-type cells. In the presence of HU, however, almost all G1 released cells were arrested in S phase.

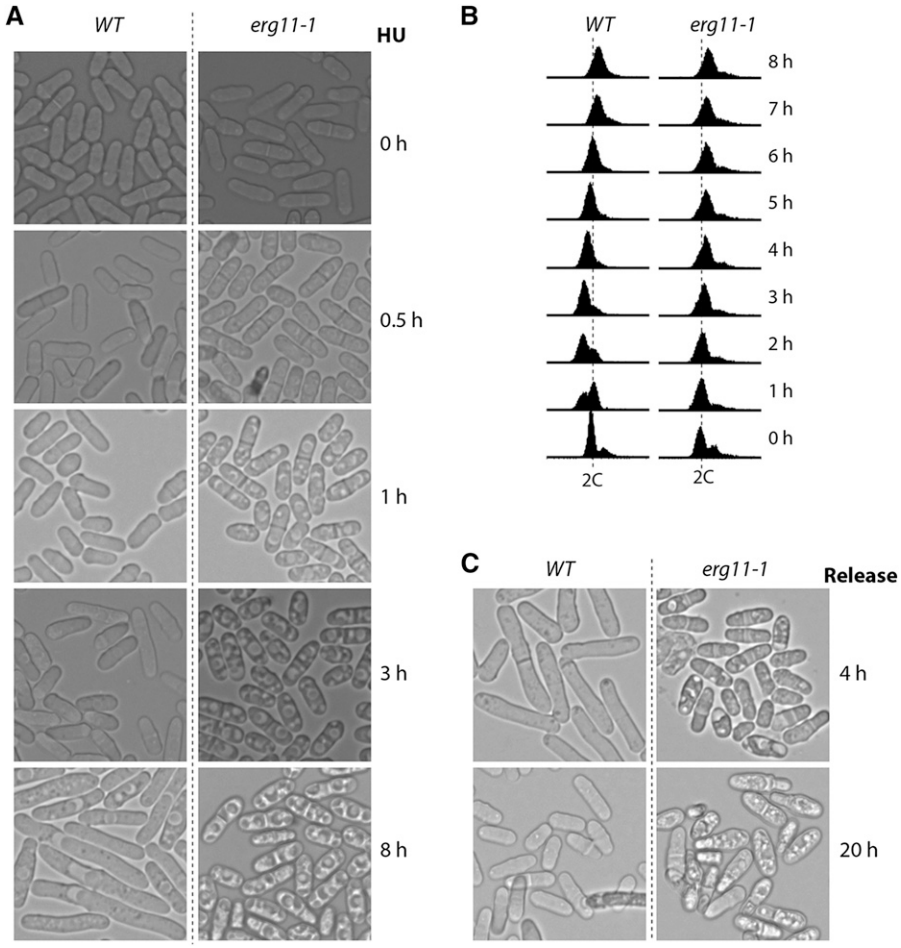

Figure 6 The cytokinesis arrest is relatively stable in comparison to the S phase arrest. Logarithmically growing wild-type and *erg11-1* cells were treated with 25 mM HU in YE6S medium at 30°. During the course of drug treatment, a small amount of the culture was removed at the indicated time points for microscopic examination (A) or cell cycle analysis by flow cytometry (B). (C) After the treatment with 25 mM HU for 8 hr, the cells were washed and released into fresh YE6S medium. During the release, the cells were examined microscopically at the indicated time points.

We then examined Cds1 phosphorylation at 3 hr after the G1 release in the presence or absence of HU. As shown in Figure S11B, Cds1 phosphorylation in G1-released-*cdc10* or wild-type cells was significantly increased in the presence of HU, although the level was slightly lower than in asynchronous cells. Under similar conditions, the phosphorylation remained low in *erg11-1*, suggesting that the mutation has a direct impact on Cds1 phosphorylation. We also examined Cds1 phosphorylation at various time points after the G1 release (Figure S11C) and found that the phosphorylation peaked at 4 hr in wild-type cells after the G1 release. However, the phosphorylation remained low in the mutant cells at all time points tested. In a separate experiment, the phosphorylation was examined at 1 hr after the G1 release and the same result was obtained (data not shown). Together, this result suggests that the *erg11-1* mutation may partially affect the Cds1 activation in the presence of HU. However, because most of the cells were stably arrested in cytokinesis, the reduced DRC signaling may contribute minimally to the HU-induced cell death.

All other known erg mutants in the ergosterol synthesis pathway are resistant or minimally sensitive to HU

An earlier report showed that a mutation in *hmg1*, which encodes the enzyme 3-hydroxy-3-methylglutaryl coenzyme A reductase within the sterol biosynthetic pathway, causes a mild defect in cytokinesis (Fang *et al.* 2009). This suggests that sterol deficiency may be the cause of the HU-induced cytokinesis arrest. To examine the sterol level in *erg11-1*, we stained the cells with the fluorescent dye filipin, a polyene antibiotic that forms a specific complex with 3-β-hydroxysterols (Wachtler *et al.* 2003). As shown in Figure 7A, the cell tips and septa where sterol is enriched could all be stained. Interestingly, although the *erg11-1* cells were also stained, the level of staining appeared to be reduced. This result showed that, consistent with the hypomorphic mutation, the sterol level might be slightly lower in *erg11-1* cells. We then examined whether other mutants in the ergosterol biosynthesis pathway, including *erg6*Δ, *erg3*Δ, and *erg4*Δ, are also sensitive to HU (Figure 7B). To our surprise, none of the tested *erg* mutants except *erg11-1* were highly sensitive. Interestingly, deletion of the nonessential enzyme Erg6, which functions upstream of Erg11, also mildly sensitized the cells to HU, although the sensitivity was not comparable to that of *erg11-1*. These results suggest that some of the enzymes are functionally redundant or products of the enzymes, particularly those near the end of the biosynthesis pathway, may replace the cellular functions of ergosterol.

Enhanced sensitivity to antifungal azoles

The results described above suggest that sterol deficiency may predispose the cells to the cytokinesis arrest and thus sensitize the cells to HU. It is also possible, although less likely, that a toxic byproduct is generated by the mutant enzyme that sensitizes the cells to HU. To investigate this possibility, we tested whether the *erg11-1* mutant could be rescued chemically by exogenously supplied ergosterol. However, after the experiment was repeated multiple times with various modifications, we found that the exogenous ergosterol could not rescue the *erg11-1* mutant. Consistent with this result, an earlier report showed that unlike *S. cerevisiae*, *S. pombe* does not take up the exogenous ergosterol supplied in the medium (Hughes *et al.* 2005). Thus, this lack of ergosterol uptake may provide an explanation for our negative results in rescuing the mutant with exogenous ergosterol.

Since Erg11 is the major target of antifungal azoles, its inhibitors are commercially available. We then tested the effect of Erg11 inhibitors on the cell growth and HU sensitivity of the *erg11-1* mutant. We reasoned that if the HU sensitivity is caused by sterol deficiency, the mutant should be more sensitive to Erg11 inhibitors, and treatment of wild-type *S. pombe* with the inhibitors should mimic the mutant effect and thus sensitize wild-type cells to HU. Standard spot assays were used to test the effects of two inhibitors clotrimazole and terbinafine (Figure 7C). We found that while wild type and checkpoint mutants such as *rad3*, *cds1*, and *chk1* had a similar drug resistance, the *erg11-1* cells were much more sensitive to the tested drugs. These results suggest that it is likely that the sterol deficiency, and not a toxic byproduct, sensitizes the *erg11-1* cells to HU. We also tested a third inhibitor itraconazole, and similar results were obtained (Figure S12A). Importantly, we found that at the minimal drug concentration that hardly affects the cell proliferation, itraconazole significantly sensitized wild-type *S. pombe* to HU (Figure S12B), which phenocopies the *erg11-1* mutation and strongly supports our conclusion that sterol deficiency sensitizes the cells to HU.

Discussion

In this paper, we show that a single G189D mutation in Erg11, an essential enzyme sterol-14α-demethylase required for ergosterol biosynthesis, significantly sensitizes *S. pombe* to chronic HU treatment. Unexpectedly, the mutant cells are likely not killed by perturbed DNA replication, but by a previously unknown mechanism involving cytokinesis arrest. We also provide several lines of evidence that the remarkable HU sensitivity is caused by sterol deficiency, which predisposes the cells to the cytokinesis arrest induced by HU. First, when cultured in rich medium, the mutant grows almost like the wild-type cells, indicating that a minimal sterol level remains for normal cell growth. Second, the genetic data suggest that the mutation is hypomorphic, which is consistent with the location of the mutation outside of the catalytic center of the enzyme and the rescuing effect of overexpressed mutant enzyme. Third, filipin staining provides direct evidence that the sterol level remains at a detectable level. Fourth, unlike the checkpoint mutants with a wild-type drug resistance, the mutant is highly sensitive to the Erg11 inhibitors. Finally, treatment of wild-type *S. pombe* with the Erg11 inhibitor itraconazole sensitizes the cells to HU, which phenocopies the *erg11-1* mutant. We believe that it is unlikely that the remarkable HU sensitivity is caused by an unknown toxin generated by the mutated enzyme. Further studies are needed to understand the exact mechanism by which sterol deficiency sensitizes *S. pombe* to chronic HU exposure.

Because Mrc1 is specifically expressed during S phase and a stable cytokinesis arrest is induced in the mutant cells, the low levels of Mrc1 protein and its phosphorylation are likely caused indirectly by the cell cycle defect. However, it remains unclear why Cds1 phosphorylation remains at a low level even when the cells were forced to enter the S phase in the presence of HU. It is possible that abundant ergosterol is required for efficient DRC signaling in fission yeast. Nevertheless, we believe that it is unlikely that the reduced DRC signaling contributes significantly to the HU-induced cell death in *erg11-1* mutant.

HU primarily targets RNR by quenching the tyrosyl free radical required for the catalysis. Consistent with this mechanism, HU arrests proliferating cells in S phase, and defects in the DRC sensitize the cells to HU, probably by aberrant mitosis and the DNA strand breaks generated at unprotected forks. However, how HU kills wild-type cells with a functional DRC is less understood. Although the DNA damage generated at HU-treated forks is believed to play an important role in the cell-killing process, recent studies suggest that HU may generate oxidative stress in *Escherichia coli* (Davies *et al.* 2009; Foti *et al.* 2012) and in *S. cerevisiae* (Chang *et al.* 2002; Han *et al.* 2010; Rowe *et al.* 2012). However, it remains unclear whether this cell-killing mechanism is conserved in all eukaryotic organisms and how this mechanism is related to the cytokinesis arrest discovered in this study. Understanding the HU-induced cytokinesis arrest may shed new light on the cytotoxicity of HU and derive new therapeutic potentials because cytokinesis has been widely exploited as an antiproliferative strategy for the development of cancer chemotherapeutics (Bathe and Chang 2010; Lee *et al.* 2012).

Cytokinesis partitions a mother cell into two daughters at the end of each cell cycle. Failure in cytokinesis results in aneuploidy and contributes to tumorigenesis (Bathe and Chang 2010; Lee *et al.* 2012). Since ergosterol is enriched in the septum, it is possible that its deficiency directly affects the cell separation process. Alternatively, a cytokinesis protein is targeted by HU. *S. pombe* offers an excellent model for dissecting the mechanisms involved in this process because conserved sets of cytokinesis proteins and pathways have been identified and functionally characterized. The septa in HU-treated *erg11-1* cells are all properly positioned in the middle of the cell and all cells contain only one septum. It is likely that HU affects late stages of cytokinesis. Testing the

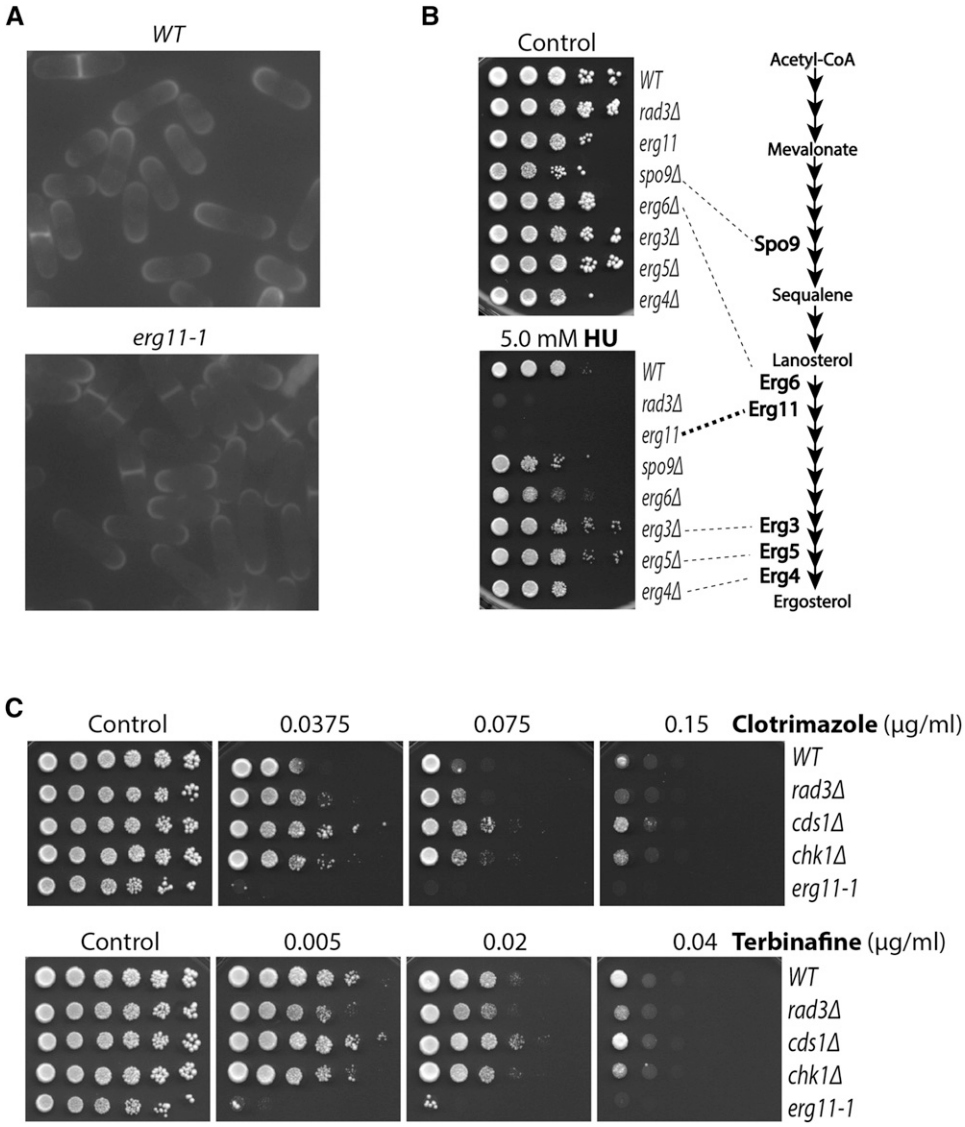

Figure 7 The *erg11-1* mutation reduces the sterol level and predisposes the cells to HU-induced cell death. (A) The sterol level in *erg11-1* cells is lower than that in wild-type cells. Logarithmically growing wild-type (top) and the *erg11-1* cells (bottom) were stained with filipin dye and examined by fluorescent microscopy. (B) The *erg11-1* cells and the cells lacking the indicated enzymes in the ergosterol synthesis pathway were tested by spot assays for HU sensitivity. (C) Sensitivity of wild-type cells and the cells with indicated mutations to the Erg11 inhibitor clotrimazole (top) and terbinafine (bottom) were examined with the standard spot assays on plates containing YE6S medium. The plates were incubated at 30° for 3 days.

relationship between the *erg11-1* mutation and a set of late stage of cytokinesis mutants such as *byr4*, *cdc16*, *dma1*, and *nuc2* with defects in septum resolution or cell separation, may pinpoint the exact step where the arrest occurs during cytokinesis (Gould and Simanis 1997; Rajagopalan *et al.* 2003). It is possible that in addition to RNR, HU may have a secondary unidentified target(s) inside the cell. For example, it has been shown that *in vitro*, HU can inhibit carbonic anhydrase and matrix metalloproteinases (Scozzafava and Supuran 2003; Temperini *et al.* 2006).

Understanding the new cell-killing mechanism of an established drug with multiple clinical implications is important for the development of novel chemotherapeutics. Since its first synthesis >150 years ago, HU has been extensively studied in both laboratories and clinics (Stevens 1999; Spivak and Hasselbalch 2011). It is a water-soluble, well-absorbed, and highly tolerable small molecule drug that has been used to treat leukemia, solid tumors, sickle cell anemia, HIV infection, psoriasis, and various other diseases. Today, it remains the staple drug in the management of sickle cell anemia and chronic myeloproliferative disorders. However, despite the strong evidence of its clinical efficacies in a wide range of disorders, its use as a reliable drug in neoplastic and nonneoplastic disorders remains limited. The main reason for this limitation is due to the side effects and incomplete understanding of the mechanism underlying the toxicities. Understanding the novel cell-killing mechanism of HU may therefore greatly improve the chemotherapies that employ HU.

Acknowledgments

We are thankful to Paul Russell, Tony Carr, and Tom Kelly for sharing the yeast strains and Michael Kemp for critical reading of the manuscript. Other members of the authors' laboratory are acknowledged for their support and help. This work was supported by National Institutes of Health R01 grant GM-110132 to Y.-j.X. and start-up funds provided by Wright State University.

Literature Cited

Ahn, J., M. Urist, and C. Prives, 2004 The Chk2 protein kinase. DNA Repair (Amst.) 3: 1039–1047.

Akerblom, L., A. Ehrenberg, A. Graslund, H. Lankinen, P. Reichard *et al.*, 1981 Overproduction of the free radical of ribonucleotide reductase in hydroxyurea-resistant mouse fibroblast 3T6 cells. Proc. Natl. Acad. Sci. USA 78: 2159–2163.

Bandhu, A., J. Kang, K. Fukunaga, G. Goto, and K. Sugimoto, 2014 Ddc2 mediates Mec1 activation through a Ddc1- or Dpb11-independent mechanism. PLoS Genet. 10: e1004136.

Bathe, M., and F. Chang, 2010 Cytokinesis and the contractile ring in fission yeast: towards a systems-level understanding. Trends Microbiol. 18: 38–45.

Becher, R., and S. G. Wirsel, 2012 Fungal cytochrome P450 sterol 14alpha-demethylase (CYP51) and azole resistance in plant and human pathogens. Appl. Microbiol. Biotechnol. 95: 825–840.

Boddy, M. N., and P. Russell, 2001 DNA replication checkpoint. Curr. Biol. 11: R953–R956.

Cai, Z., N. H. Chehab, and N. P. Pavletich, 2009 Structure and activation mechanism of the CHK2 DNA damage checkpoint kinase. Mol. Cell 35: 818–829.

Chang, M., M. Bellaoui, C. Boone, and G. W. Brown, 2002 A genome-wide screen for methyl methanesulfonate-sensitive mutants reveals genes required for S phase progression in the presence of DNA damage. Proc. Natl. Acad. Sci. USA 99: 16934–16939.

Chen, P., C. Luo, Y. Deng, K. Ryan, J. Register *et al.*, 2000 The 1.7 A crystal structure of human cell cycle checkpoint kinase Chk1: implications for Chk1 regulation. Cell 100: 681–692.

Choy, B. K., G. A. McClarty, A. K. Chan, L. Thelander, and J. A. Wright, 1988 Molecular mechanisms of drug resistance involving ribonucleotide reductase: hydroxyurea resistance in a series of clonally related mouse cell lines selected in the presence of increasing drug concentrations. Cancer Res. 48: 2029–2035.

Ciccia, A., and S. J. Elledge, 2010 The DNA damage response: making it safe to play with knives. Mol. Cell 40: 179–204.

Davies, B. W., M. A. Kohanski, L. A. Simmons, J. A. Winkler, J. J. Collins *et al.*, 2009 Hydroxyurea induces hydroxyl radical-mediated cell death in Escherichia coli. Mol. Cell 36: 845–860.

Ehrenberg, A., and P. Reichard, 1972 Electron spin resonance of the iron-containing protein B2 from ribonucleotide reductase. J. Biol. Chem. 247: 3485–3488.

Elledge, S. J., Z. Zhou, and J. B. Allen, 1992 Ribonucleotide reductase: regulation, regulation, regulation. Trends Biochem. Sci. 17: 119–123.

Enoch, T., A. M. Carr, and P. Nurse, 1992 Fission yeast genes involved in coupling mitosis to completion of DNA replication. Genes Dev. 6: 2035–2046.

Espenshade, P. J., and A. L. Hughes, 2007 Regulation of sterol synthesis in eukaryotes. Annu. Rev. Genet. 41: 401–427.

Fang, Y., K. Imagawa, X. Zhou, A. Kita, R. Sugiura *et al.*, 2009 Pleiotropic phenotypes caused by an opal nonsense mutation in an essential gene encoding HMG-CoA reductase in fission yeast. Genes Cells 14: 759–771.

Fernandez Sarabia, M. J., C. McInerny, P. Harris, C. Gordon, and P. Fantes, 1993 The cell cycle genes cdc22+ and suc22+ of the fission yeast Schizosaccharomyces pombe encode the large and small subunits of ribonucleotide reductase. Mol. Gen. Genet. 238: 241–251.

Foti, J. J., B. Devadoss, J. A. Winkler, J. J. Collins, and G. C. Walker, 2012 Oxidation of the guanine nucleotide pool underlies cell death by bactericidal antibiotics. Science 336: 315–319.

Furuya, K., and A. M. Carr, 2003 DNA checkpoints in fission yeast. J. Cell Sci. 116: 3847–3848.

Furuya, K., M. Poitelea, L. Guo, T. Caspari, and A. M. Carr, 2004 Chk1 activation requires Rad9 S/TQ-site phosphorylation to promote association with C-terminal BRCT domains of Rad4-TOPBP1. Genes Dev. 18: 1154–1164.

Gould, K. L., and V. Simanis, 1997 The control of septum formation in fission yeast. Genes Dev. 11: 2939–2951.

Han, T. X., X. Y. Xu, M. J. Zhang, X. Peng, and L. L. Du, 2010 Global fitness profiling of fission yeast deletion strains by barcode sequencing. Genome Biol. 11: R60.

Han, X., J. Tang, J. Wang, F. Ren, J. Zheng *et al.*, 2016 Conformational change of human checkpoint kinase 1 (Chk1) induced by DNA damage. J. Biol. Chem. 291: 12951–12959.

Hu, J., L. Sun, F. Shen, Y. Chen, Y. Hua *et al.*, 2012 The intra-S phase checkpoint targets Dna2 to prevent stalled replication forks from reversing. Cell 149: 1221–1232.

Hughes, A. L., B. L. Todd, and P. J. Espenshade, 2005 SREBP pathway responds to sterols and functions as an oxygen sensor in fission yeast. Cell 120: 831–842.

Ivanova, T., I. Alves-Rodrigues, B. Gomez-Escoda, C. Dutta, J. A. Decaprio *et al.*, 2013 The DNA damage and the DNA replication checkpoints converge at the MBF transcription factor. Mol. Biol. Cell 24: 3350–3357.

Johnson, A. E., D. McCollum, and K. L. Gould, 2012 Polar opposites: fine-tuning cytokinesis through SIN asymmetry. Cytoskeleton 69: 686–699.

Kim, D. U., J. Hayles, D. Kim, V. Wood, H. O. Park *et al.*, 2010 Analysis of a genome-wide set of gene deletions in the fission yeast Schizosaccharomyces pombe. Nat. Biotechnol. 28: 617–623.

Krakoff, I. H., N. C. Brown, and P. Reichard, 1968 Inhibition of ribonucleoside diphosphate reductase by hydroxyurea. Cancer Res. 28: 1559–1565.

Lamb, D. C., D. E. Kelly, K. Venkateswarlu, N. J. Manning, H. F. Bligh *et al.*, 1999 Generation of a complete, soluble, and catalytically active sterol 14 alpha-demethylase-reductase complex. Biochemistry 38: 8733–8738.

Lee, I. J., V. C. Coffman, and J. Q. Wu, 2012 Contractile-ring assembly in fission yeast cytokinesis: recent advances and new perspectives. Cytoskeleton (Hoboken) 69: 751–763.

Limbo, O., M. E. Porter-Goff, N. Rhind, and P. Russell, 2011 Mre11 nuclease activity and Ctp1 regulate Chk1 activation by Rad3ATR and Tel1ATM checkpoint kinases at double-strand breaks. Mol. Cell. Biol. 31: 573–583.

Lindsay, H. D., D. J. Griffiths, R. J. Edwards, P. U. Christensen, J. M. Murray *et al.*, 1998 S-phase-specific activation of Cds1 kinase defines a subpathway of the checkpoint response in Schizosaccharomyces pombe. Genes Dev. 12: 382–395.

Lopes, M., C. Cotta-Ramusino, A. Pellicioli, G. Liberi, P. Plevani *et al.*, 2001 The DNA replication checkpoint response stabilizes stalled replication forks. Nature 412: 557–561.

Lopez-Mosqueda, J., N. L. Maas, Z. O. Jonsson, L. G. Defazio-Eli, J. Wohlschlegel *et al.*, 2010 Damage-induced phosphorylation of Sld3 is important to block late origin firing. Nature 467: 479–483.

Lowndes, N. F., C. J. McInerny, A. L. Johnson, P. A. Fantes, and L. H. Johnston, 1992 Control of DNA synthesis genes in fission yeast by the cell-cycle gene cdc10+. Nature 355: 449–453.

Moreno, S., A. Klar, and P. Nurse, 1991 Molecular genetic analysis of fission yeast Schizosaccharomyces pombe. *Methods Enzymol.* 194: 795–823.

Nestoras, K., A. H. Mohammed, A. S. Schreurs, O. Fleck, A. T. Watson *et al.*, 2010 Regulation of ribonucleotide reductase by Spd1 involves multiple mechanisms. Genes Dev. 24: 1145–1159.

Noguchi, E., C. Noguchi, L. L. Du, and P. Russell, 2003 Swi1 prevents replication fork collapse and controls checkpoint kinase Cds1. Mol. Cell. Biol. 23: 7861–7874.

Nordlund, P., and P. Reichard, 2006 Ribonucleotide reductases. Annu. Rev. Biochem. 75: 681–706.

Porollo, A., R. Adamczak, and J. Meller, 2004 POLYVIEW: a flexible visualization tool for structural and functional annotations of proteins. Bioinformatics 20: 2460–2462.
Rajagopalan, S., V. Wachtler, and M. Balasubramanian, 2003 Cytokinesis in fission yeast: a story of rings, rafts and walls. Trends Genet. 19: 403–408.
Rowe, L. A., N. Degtyareva, and P. W. Doetsch, 2012 Yap1: a DNA damage responder in Saccharomyces cerevisiae. Mech. Ageing Dev. 133: 147–156.
Saka, Y., and M. Yanagida, 1993 Fission yeast cut5+, required for S phase onset and M phase restraint, is identical to the radiation-damage repair gene rad4+. Cell 74: 383–393.
Scozzafava, A., and C. T. Supuran, 2003 Hydroxyurea is a carbonic anhydrase inhibitor. Bioorg. Med. Chem. 11: 2241–2246.
Sogo, J. M., M. Lopes, and M. Foiani, 2002 Fork reversal and ssDNA accumulation at stalled replication forks owing to checkpoint defects. Science 297: 599–602.
Spivak, J. L., and H. Hasselbalch, 2011 Hydroxycarbamide: a user's guide for chronic myeloproliferative disorders. Expert Rev. Anticancer Ther. 11: 403–414.
Stevens, M. R., 1999 Hydroxyurea: an overview. J. Biol. Regul. Homeost. Agents 13: 172–175.
Stracker, T. H., S. S. Couto, C. Cordon-Cardo, T. Matos, and J. H. Petrini, 2008 Chk2 suppresses the oncogenic potential of DNA replication-associated DNA damage. Mol. Cell 31: 21–32.
Strushkevich, N., S. A. Usanov, and H. W. Park, 2010 Structural basis of human CYP51 inhibition by antifungal azoles. J. Mol. Biol. 397: 1067–1078.
Tanaka, K., M. N. Boddy, X. B. Chen, C. H. McGowan, and P. Russell, 2001 Threonine-11, phosphorylated by Rad3 and atm in vitro, is required for activation of fission yeast checkpoint kinase Cds1. Mol. Cell. Biol. 21: 3398–3404.
Temperini, C., A. Innocenti, A. Scozzafava, and C. T. Supuran, 2006 N-hydroxyurea: a versatile zinc binding function in the design of metalloenzyme inhibitors. Bioorg. Med. Chem. Lett. 16: 4316–4320.
Turi, T. G., and J. C. Loper, 1992 Multiple regulatory elements control expression of the gene encoding the Saccharomyces cerevisiae cytochrome P450, lanosterol 14 alpha-demethylase (ERG11). J. Biol. Chem. 267: 2046–2056.
Wachtler, V., S. Rajagopalan, and M. K. Balasubramanian, 2003 Sterol-rich plasma membrane domains in the fission yeast Schizosaccharomyces pombe. J. Cell Sci. 116: 867–874.
Xu, Y. J., 2016 Inner nuclear membrane protein Lem2 facilitates Rad3-mediated checkpoint signaling under replication stress induced by nucleotide depletion in fission yeast. Cell. Signal. 28: 235–245.
Xu, Y. J., and T. J. Kelly, 2009 Autoinhibition and autoactivation of the DNA replication checkpoint kinase Cds1. J. Biol. Chem. 284: 16016–16027.
Xu, Y. J., M. Davenport, and T. J. Kelly, 2006 Two-stage mechanism for activation of the DNA replication checkpoint kinase Cds1 in fission yeast. Genes Dev. 20: 990–1003.
Yue, M., A. Singh, Z. Wang, and Y. J. Xu, 2011 The phosphorylation network for efficient activation of the DNA replication checkpoint in fission yeast. J. Biol. Chem. 286: 22864–22874.
Yue, M., L. Zeng, A. Singh, and Y. J. Xu, 2014 Rad4 mainly functions in Chk1-mediated DNA damage checkpoint pathway as a scaffold protein in the fission yeast Schizosaccharomyces pombe. PLoS One 9: e92936.
Zegerman, P., and J. F. Diffley, 2010 Checkpoint-dependent inhibition of DNA replication initiation by Sld3 and Dbf4 phosphorylation. Nature 467: 474–478.

Communicating editor: J. A. Nickoloff

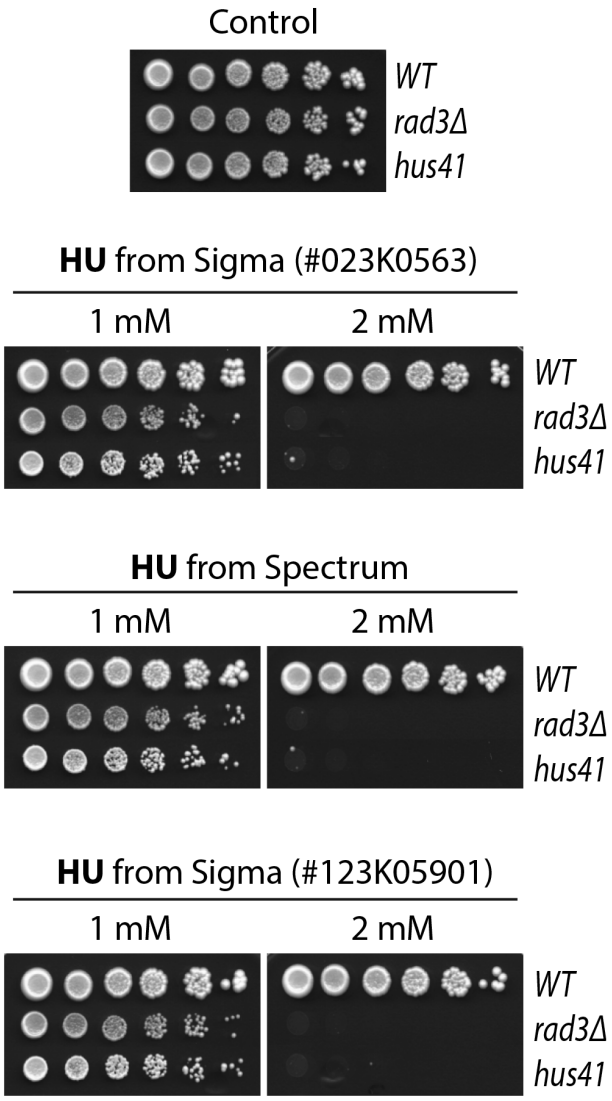

Figure S1. HU from various manufacturers and batch numbers showed a similar cell-killing effect to *hus41* mutant. HU sensitivity of wild type, *rad3* and *hus41* mutant cells was assessed by standard spot assays using HU from Sigma with different batch numbers (Top and bottom panels) or Spectrum (middle panel).

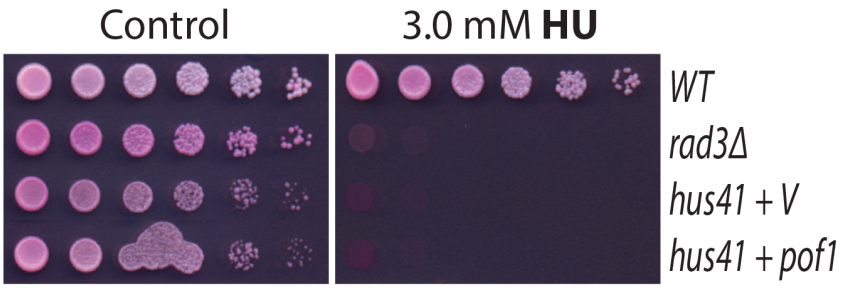

Figure S2. Expression of wild type Pof1 in *hus41* could not rescue the HU sensitivity. HU sensitivity of wild type, *rad3*, *hus41* carrying an empty vector (V) or the same vector expressing Pof1 was assessed by standard spot assays. 2 x 10^7 cells/ml of logarithmically growing *S. pombe* were diluted in five-fold steps and spotted onto YE6S plates as the control or YE6S plates containing 3.0 mM HU. The plates were incubated at 30˚C for 3 days. The lethality dye Phloxin B was added to the medium in this experiment. The result showed that expression of Pof1 cannot rescue *hus41*, suggesting that the *pof1* is not mutated in the *hus41* mutant.

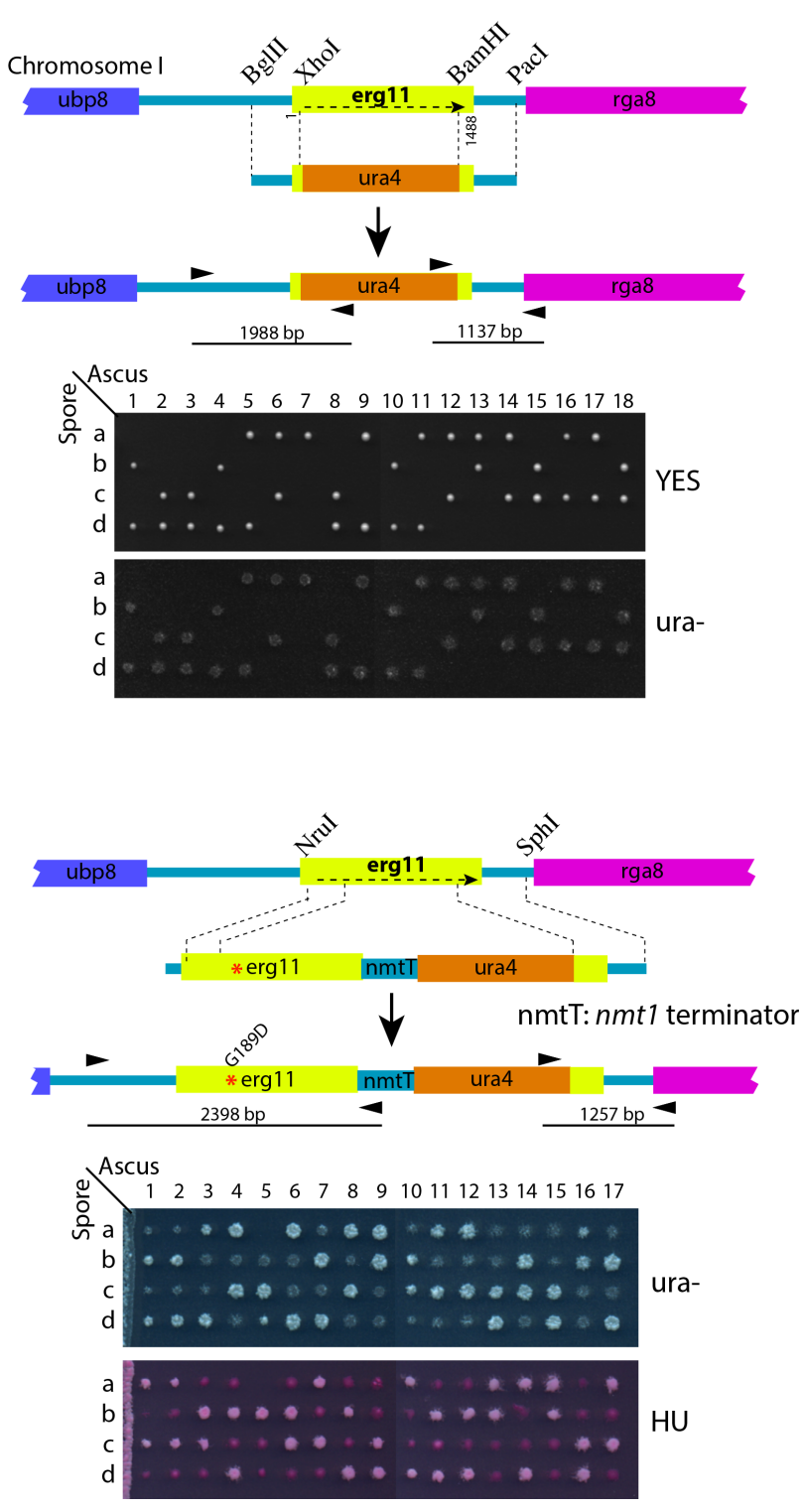

Figure S3. Diagrams showing the methods used for deletion of *erg11* gene (A) or integration of the *erg11-1* mutation at the genomic locus (B). **(A)** The *erg11* gene was deleted by replacing with the *ura4* marker. The XhoI and BamHI restriction sites were generated by mutational PCR in the *erg11* ORF in pYJ1519 between 79 bp to 2568 bp from the start codon. After digestion with XhoI and BamHI, the 2489 bp region of *erg11* ORF was replaced with an *ura4* marker DNA to make the deletion construct pYJ1526. The deletion construct was digested with BglII and PacI to isolate the 3818 bp gene replacement fragment, which was transformed into the wild type diploid strain YJ18. The colonies grown on EMM6S[ura$^-$] plates were screened by colony PCRs with the primers shown as the short arrows to confirm the correct integration at the 5' and 3' ends. The confirmed diploid strain was saved as YJ1245 and the essentiality of *erg11* was demonstrated by tetrad dissection and subsequent replica plating (lower panels). (**B**) Integration of the *erg11-1* mutation (indicated by the red asterisk) at the genomics locus was achieved in the wild type diploid strain YJ18. The mutated *erg11* gene is under the control of its own promoter and an nmt1 terminator (nmtT). For the convenience of positive selection, the mutated *erg11* was fused with the *ura4* marker. The colonies grown on plates lacking uracil were screened by colony PCR to confirm the correct integration. After tetrad dissection, all integrants carrying the *ura4* markers were sensitive to HU (lower panels), which shows that the *erg11-1* mutation causes a remarkable HU sensitivity.

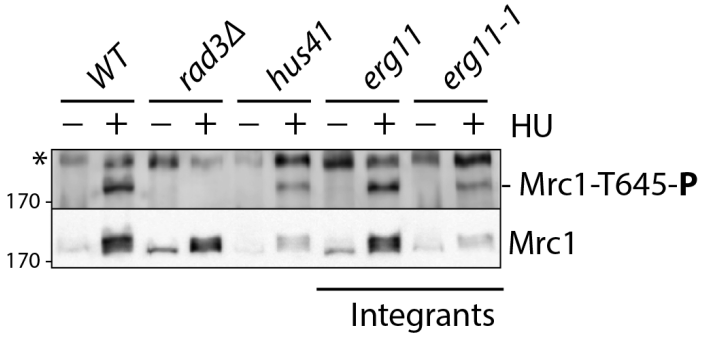

Figure S4. Phosphorylation of Mrc1 in the integrated *erg11-1* mutant is essentially the same as that in the screened *hus41* cells in the presence of HU. Wild type, *rad3*, *hus41* and the integrant of wild type *erg11* or *erg11-1* mutation were treated with (+) or without (-) 15 mM HU for 3 h. Phosphorylation of Mrc1 was examined by Western blotting using phospho-specific antibodies (upper panel) as described in Materials and Methods. The same blot was stripped and reprobed using anti-Mrc1 antibodies to determine the relative levels of Mrc1 protein (lower panel). The results showed that phosphorylation of Mrc1 in HU-treated *erg11-1* mutant is indistinguishable from that in the *hus41* mutant.

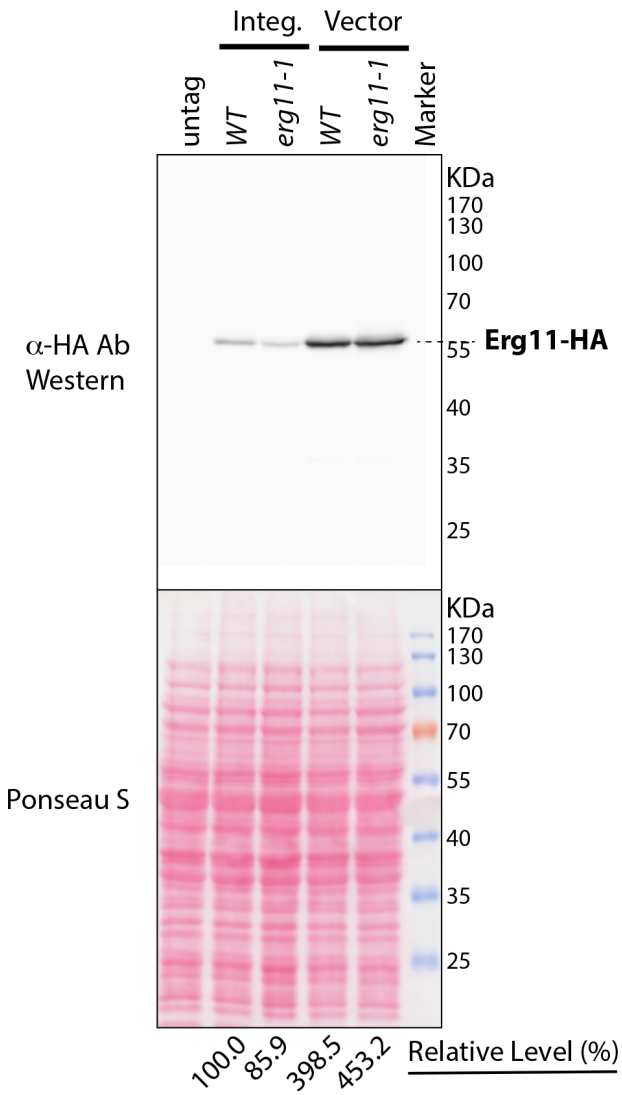

Figure S5. The level of Erg11 expressed from a vector is ~ 4 fold higher than that expressed from the genomic locus. Wild type Erg11 and its G189D mutant form were tagged with a triple HA epitope at the C-terminus and expressed under the control of its own promoter from the genomic locus (integ.) or on a vector in *erg11* deletion cells as indicated on the top. The strains with integrated expression cassettes at the genomic locus and expression vectors were made following the method diagramed in Figure S3. Equal numbers of logarithmically growing cells were fixed in 15% TCA and then lysed by mini-bead beater. After separation by a 10% SDS PAGE gel, the protein samples were transferred to a nitrocellulose membrane and stained with Ponceau S (lower panel). The membrane was then probed with anti-HA antibody for the tagged protein (upper panel). The parental strain used for integration of the HA-tagged Erg11 expression cassette was used as the negative control (first lane on the left). The Western blotting result showed that only one band corresponding to the expected size of Erg11 was detected, which confirms the correct tagging. The intensities of the bands were quantitated by ImageGauge and are shown on the bottom with the level of wild type enzyme expressed from genomic locus being set as 100%. The protein levels of wild type and mutant Erg11 expressed from the genomic locus are usually similar although the mutant protein (3rd lane from the left) appears to be less than the wild type enzyme (2nd lane from the left) in this specific blot.

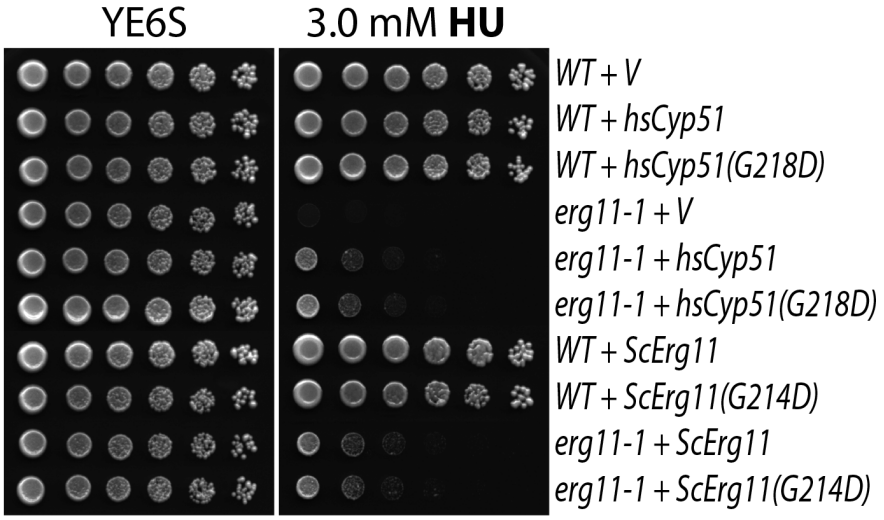

Figure S6. Similar to the wild type enzymes, overexpression of human CYP51(G218D) and *S. cerevisiae* Erg11(G214D) in *S. pombe* partially rescued the *erg11-1* mutant. The highly conserved glycine residue in the human Cyp51 and *S. cerevisae* Erg11 (Figure 1E) was mutated to aspartic acid similar to the *erg11-1* mutation by mutational PCR to make the expression vectors pYJ1656 and pYJ1657, respectively (see Table S2). The plasmids were introduced into wild type (WT) or *erg11-1 S. pombe* cells and the drug sensitivity was determined by standard spot assay. V indicates an empty vector control.

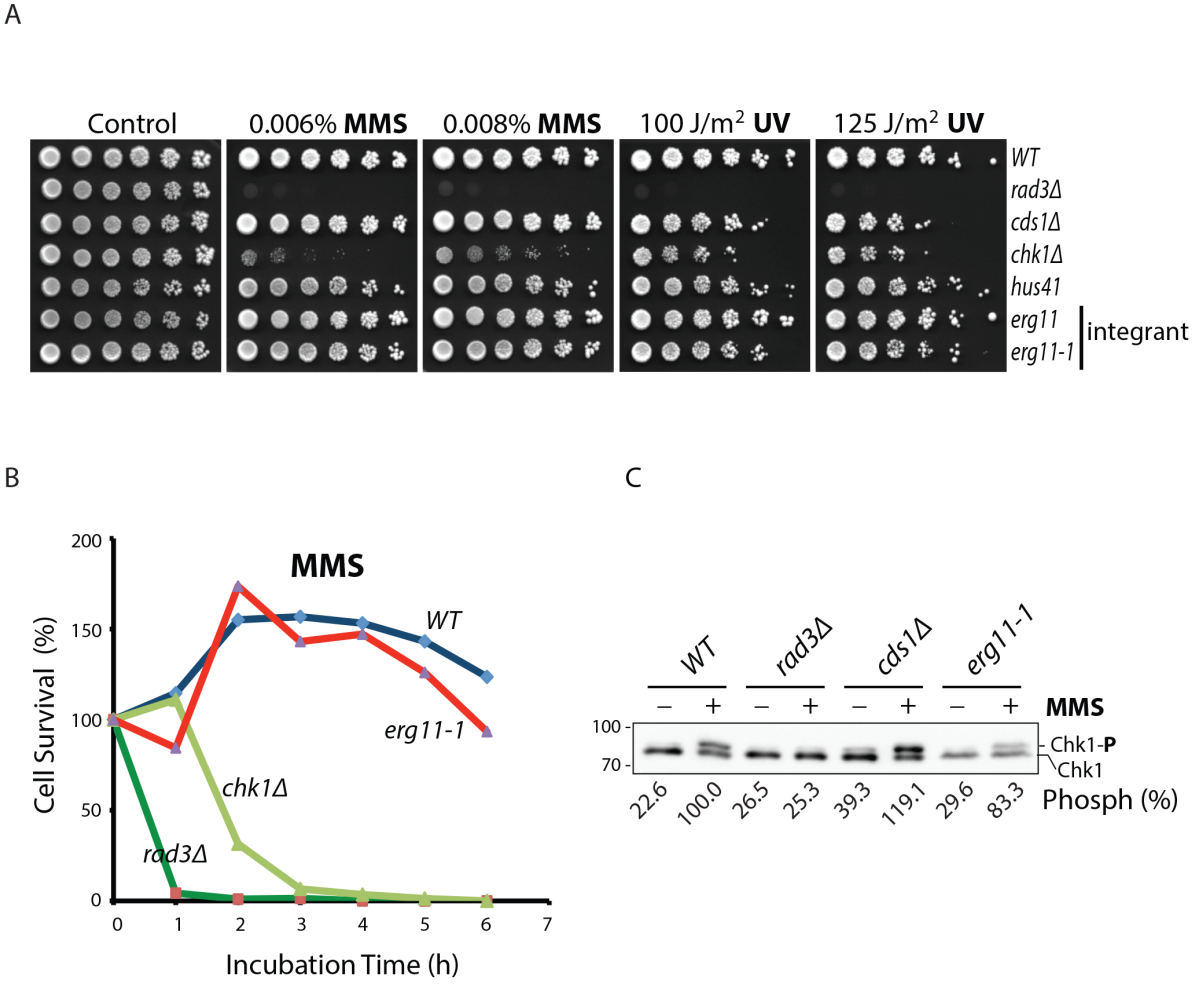

Figure S7. The *erg11-1* mutant is minimally sensitive to DNA damage caused by MMS or UV. (A) The sensitivity of wild type, *hus41* and the cells containing the indicated mutations to MMS or UV at the indicated doses was determined by standard spot assay as described in Figure 1A. **(B)** The sensitivity of wild type, *rad3*, *chk1* and *erg11-1* mutant cells to acute MMS treatment. After MMS was added to the cultures to the final concentration of 0.01%, equal amount of the culture was removed at the indicated time points, diluted 1000 fold and spread on YE6S plates to allow the cells to recover at 30˚C for 3 days. The colonies formed from the recovered cells were counted and presented as the percentages relative to the untreated cultures. (**C**) The Chk1-mediated DNA damage checkpoint response is not significantly affected in the *erg11-1* mutant. Wild type cells and mutant cells were treated with (+) or without (-) 0.01% MMS for 1 h at 30˚C for 60 min. Phosphorylation of Chk1 by Rad3 was determined by standard mobility shift assay as described in Materials and Methods. The relative levels of Chk1 phosphorylated Chk1 were quantitated by ImageGauge and shown on the bottom.

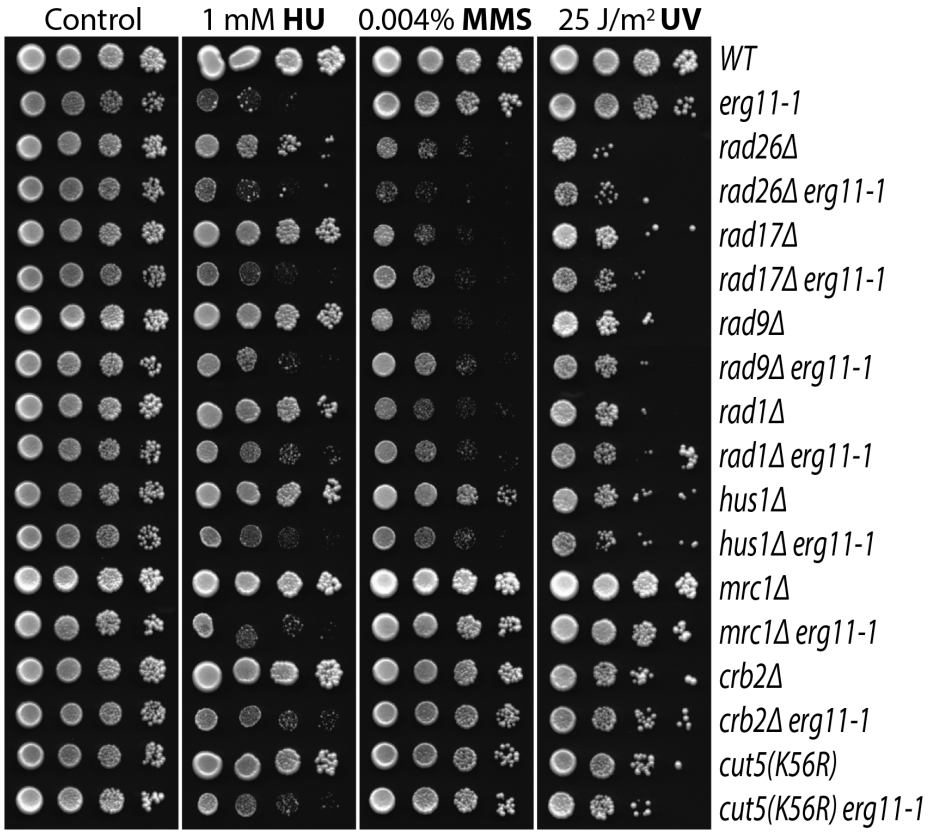

Figure S8. Dominance of *erg11-1* mutation over the checkpoint mutant in sensitizing the cells to HU, MMS and UV. The *erg11-1* mutation was crossed into the indicated checkpoint mutants. The resulting double mutants were tested by standard spot assays for the sensitivity to HU, MMS and UV at the indicated doses and compared to that of the single mutants. Cut5 is also called Rad4. It is the ortholog of *S. cerevisae* Dpb11 and mammalian TopBP1 in *S. pombe*. The previously described *cut5(K56R)* mutant has a specific defect in the DDC (YUE *et al*. 2014).

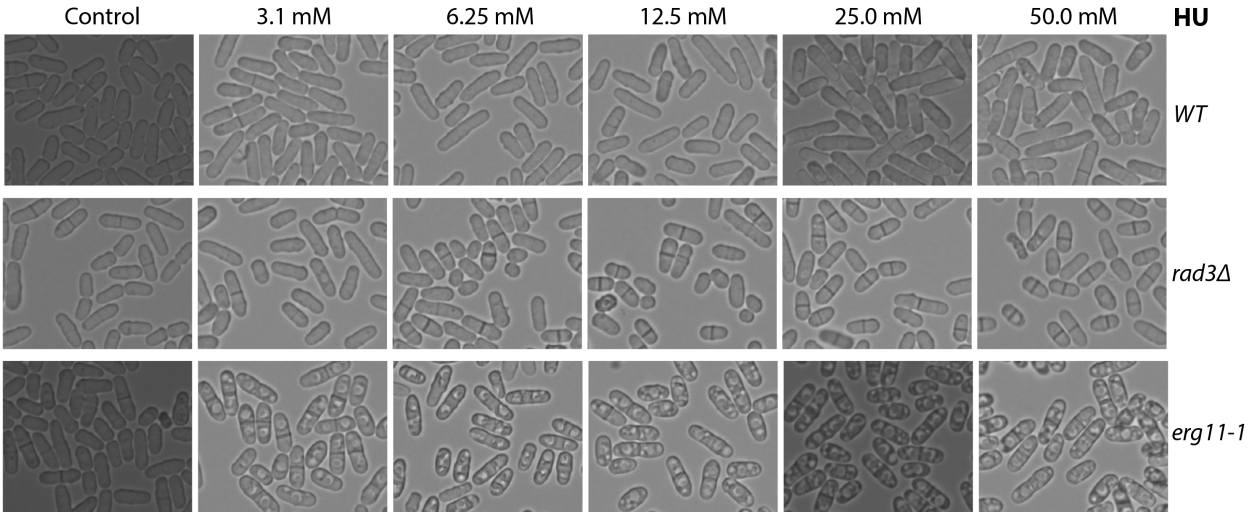

Figure S9. HU generates stress in *erg11-1* cells at a wide-range of concentrations. Wild type (top panels), *rad3* (middle panels), and the *erg11-1* (bottom panels) cells were treated with the increasing concentrations of HU for 3 h and then examined microscopically. Control indicates untreated cells. The septum and enlarged nucleus become noticeable in bright fields after treatment with 3.1 to 50.0 mM HU.

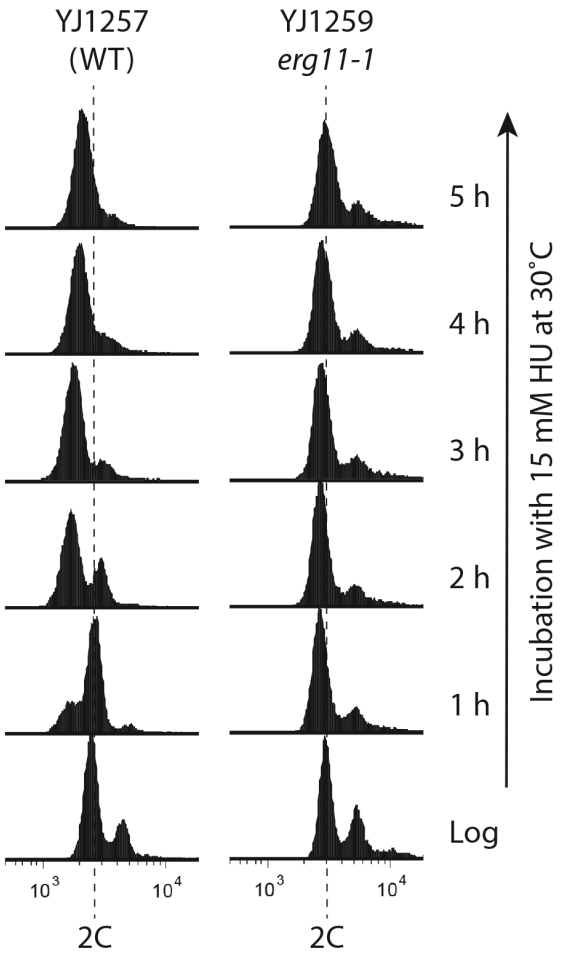

Figure S10. The *erg11-1* mutant cells were arrested at G2/M, not the S phase, in the presence of HU. The logarithmically growing wild type and the *erg11-1* mutant cells were incubated in YE6S medium containing 15 mM HU. Every hour during the HU treatment, aliquots of the cultures were removed and the cells fixed in 70% ethanol. The fixed cell samples were analyzed by flow cytometer as described in the Materials and Methods. Dash lines indicate the cells with a 2C DNA content or cells at G2/M phase. During the course of HU treatment, phosphorylation of Cds1 was examined by Western blotting using phosphor-specific antibody (see Figure 2E).

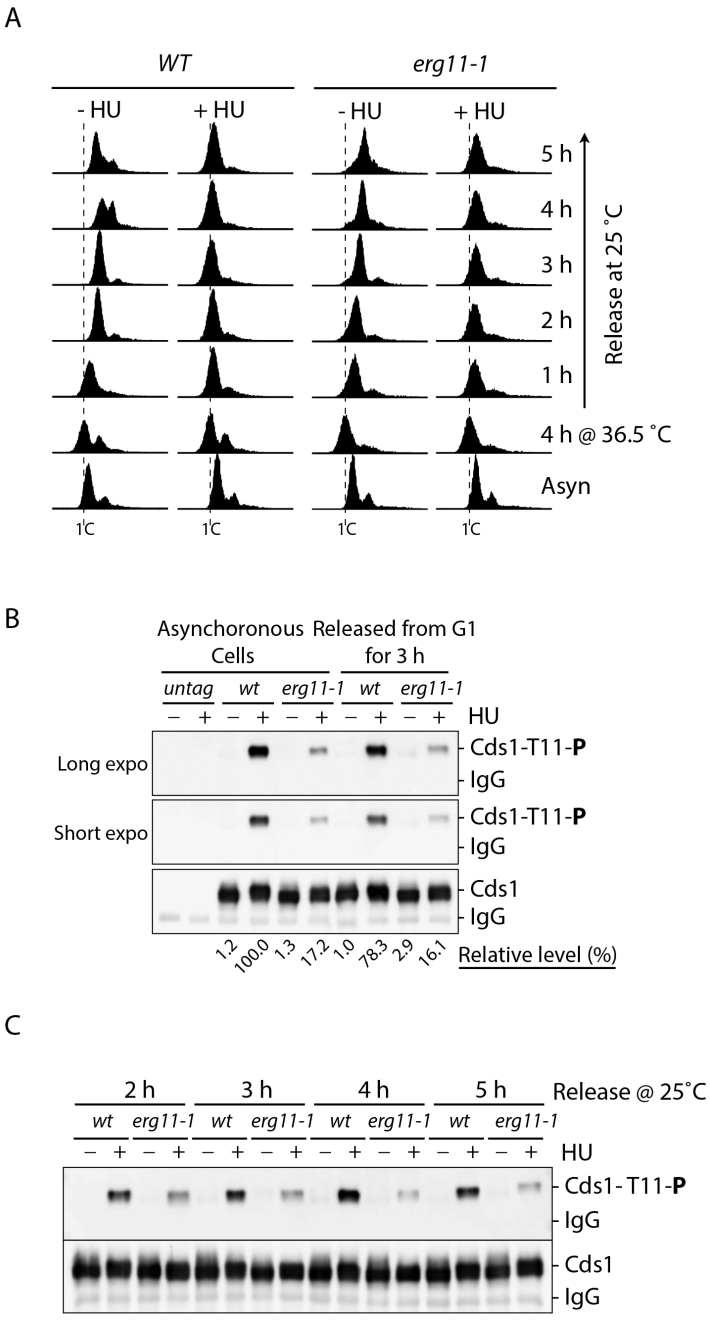

Figure S11. The partial defect in Cds1 activation may not be caused by an indirect cell cycle effect. **(A)** The *cdc10-129* cells (labeled as WT cells) or the *cdc10-129 erg11-1* double mutant (labeled as *erg11-1* cells) cells were cultured at 36.5˚C for 4 h to arrest the cells in G1 and then released into S phase by culturing at the permissive temperature 25˚C in the presence (+) or absence (-) of 15 mM HU. The cell cycle progression was monitored by flow cytometry. (**B**) Phosphorylation of Cds1 IPed from the asynchronous cultures treated with (+) or without (-) HU at 25˚C for 3 h (the first six lanes on the left). The G1-blocked cells (four lanes on the right) released at 25˚C in the presence (+) or absence (-) of HU for 3 h were collected for examination of Cds1 phosphorylation as described in Figure 2D. Longer and shorter exposures of the Cds1 phosphorylation Western blotting are shown in the top and middle panel, respectively. The relative levels of Cds1 phosphorylation are shown on the bottom. (**C**) The G1 blocked cells were released at 25˚C into S phase in the presence (+) or absence (-) of HU. During the course of release, Cds1 phosphorylation was examined at the indicated time points.

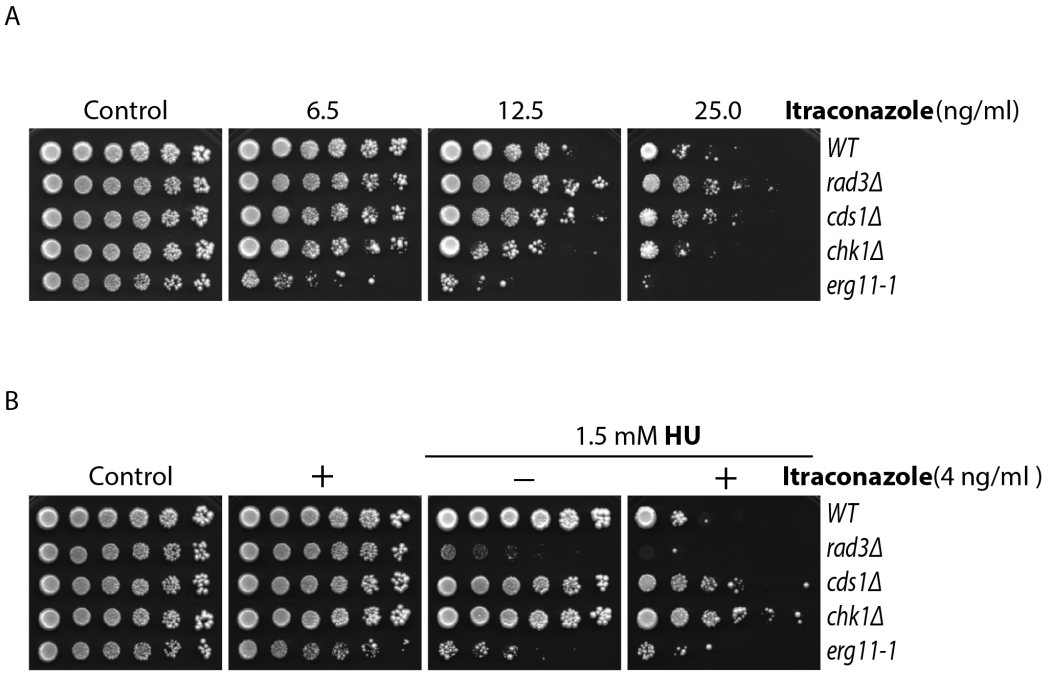

Figure S12. The Erg11 inhibitor Itraconazole significantly sensitizes wild type *S. pombe* to HU. (A) The *erg11-1* mutant is highly sensitive to Itraconazole. Wild type cells and the cells with the mutations indicated on the right were spotted on YE6S (control) or YE6S plates containing the increasing concentrations of Itraconazole. The plates were incubated at 30˚C for 3 days and then photographed. **(B)** At the minimal concentration that hardly affects the cell growth, Itraconazole significantly sensitizes wild type *S. pombe* to HU, which phenocopies the *erg11-1* mutation. Wild type and the mutant cells were spotted on YE6S (control) or YE6S plates with (+) or without (-) 4 ng/ml Itraconazole as in A. HU was also added to the two plates on the right at 1.5 mM.

Table S1. List of *S. pombe* strains used in this study.

Strain	Genotype	Sources
TK1	*h⁻*	T. Kelly lab
YJ18	*h⁻/h⁺ leu1-32/leu1-32 ura4-D18/ura4-D18 ade6-M210/ade6-M216*	Y.J. Xu lab
TK48	*h⁻ leu1-32 ade6-M216*	T. Kelly lab
NR1826	*h⁻ Δrad3::ura4 leu1-32 ura4-D18 ade6*	P. Russell lab
TK197	*h⁺ Δchk1::ura4 leu1-32 ura4-D18 ade6-M210*	T. Kelly lab
GBY191	*h⁺ Δcds1::ura4 leu1-32 ura4-D18 ade6*	T. Kelly lab
YJ1284	*h⁺ hus41[erg11(G189D)]*	This study
YJ1245	*h⁻/h⁺ Δerg11::ura4/erg11 leu1-32/leu1-32 ura4-D18/ura4-D18 ade6-M210/ade6-M216*	This study
YJ374	*h⁺ cds1-6his2HA leu1-32 ura4-D18 ade6-D216*	Y.J. Xu lab
YJ1257	*h⁺ erg11:ura4 cds1-6his2HA leu1-32 ura4-D18 ade6*	This study
YJ1259	*h⁺ erg11(G189D):ura4 cds1-6his2HA leu1-32 ura4-D18 ade6*	This study
YJ1298	*h⁺ erg11(G189D):KanR leu1-32 ura4-D18 ade6-M216*	This study
YJ1272	*h⁺ erg11(G189D):KanR chk1-9myc2HA6his:ura⁺*	This study
FY13123	*h⁺ Δspo9::ura4 leu1-32 ura4-D18 ade6-M216*	YGRC, Japan
FY17338	*h⁻ Δerg3::ura4 leu1-32 ura4-D18*	YGRC, Japan
FY17340	*h⁻ Δerg4::ura4 leu1-32 ura4-D18*	YGRC, Japan
FY17341	*h⁻ Δerg5::ura4 leu1-32 ura4-D18*	YGRC, Japan
FY17342	*h⁻ Δerg6::ura4 leu1-32 ura4-D18*	YGRC, Japan
TK198	*h⁻ Δrad26::ura4 leu1-32 ura4-D18 ade6-704*	T. Kelly lab
TK193	*h⁺ Δrad17::ura4 leu1-32 ura4-D18 ade6-M216*	T. Kelly lab
TK106	*h⁻ Δrad9::ura4 leu1-32 ura4-D18 ade6-704*	T. Kelly lab
TK194	*h⁺ Δrad1::ura4 leu1-32 ura4-D18 ade6-M210*	T. Kelly lab
1380	*h⁺ Δhus1::LEU2 leu1-32 ura4-D18 ade6-M210*	A. Carr lab
YJ15	*h⁺ ΔΔmrc1::ura4 leu1-32 ura4-D18 ade6-M210*	Y.J. Xu lab
FG2216	*h⁺ Δcrb2::ura4 leu1-32 ura4-D18*	P. Russell lab
YJ1307	*h⁻ cut5(K56R):LEU2 leu1-32 ura4-D18 ade6*	Y.J. Xu lab
YJ1453	*h⁺ Δerg11::ura4+[prom-erg11-3HA/LEU2] leu1-32 ura4-D18 ade6*	Y.J. Xu lab
YJ1454	*h⁺ Δerg11::ura4+[prom-erg11(G189D)-3HA/LEU2] leu1-32 ura4-D18 ade6*	Y.J. Xu lab
YJ1455	*h⁺ erg11-3HA:ura4+(int) leu1-32 ura4-D18 ade6-M216*	Y.J. Xu lab
YJ1456	*h⁺ erg11(G189D)-3HA:ura4+(int) leu1-32 ura4-D18 ade6-M216*	Y.J. Xu lab

Table S2. List of plasmids used in this study.

Name	**Description**	**Sources**
pYJ1519	*prom-erg1/LEU2*	This study
pYJ1520	*prom-erg11(G189D)/LEU2*	This study
pYJ1526	*prom-Δerg11::ura4+(XhoI-BamHI)/LEU2*	This study
pYJ1543	*nmt1-scErg11/LEU2*	This study
pYJ1546	*nmt1-hsCyp51/LEU2*	This study
pYJ1656	*nmt1-hsCyp51(G218D)/LEU2*	This study
pYJ1546	*nmt1-scErg11(G214D)/LEU2*	This study
pYJ1544	*prom-erg11-3HA/LEU2*	This study
pYJ1659	*prom-erg11(G189D)-3HA/LEU2*	This study

Table S3. List of PCR and sequencing primers used in this study.

Name	**Sequence (5´ -> 3´)**	**Note**
SpErg11(P)SacI-f	GTATGAGCTCGGTCCAATGGACGTG	Gene cloning
SpErg11(T)SphI-b	TCAAGCATGCCAAAAGTATCCAG	Gene cloning
Erg11(392-411)f	TCAAATCTGGTCTTGGCTTC	Sequencing
Erg11(527-508)b	GGCATGGTCTTCAGCAAATC	Sequencing
Erg11(1033-52)f	GAAACTCTTAGACTCCATCC	Sequencing
ScErg11(XhoI)f	TAATCTCGAG**ATG**TCTGCTACCAAGTCAATC	Gene cloning
ScErg11(XmaI)b	GTTACCCGGG**TTA**GATCTTTTGTTCTGG	Gene cloning
HsCyp51(XhoI)f	GGCGCTCGAG**ATG**CTGCTGCTGGGCTTGCTG	Gene cloning
HsCyp51(XmaI)b	GCAACCCGGG**TCA**TTTTGATCTTCGTTTG	Gene cloning
Ura4-b2	CTACCAATTCTAAGATTTCGGATTTC	Colony PCR
3´ura4	GCAATTTCTATGCGCACCCGTTCTCGGAGC	Colony PCR
nmtTERM-r	GGGCTTCCATAGTTTGAAAG	Colony PCR